# Altered reactivity to threatening stimuli in *Drosophila* models of Parkinson's disease, revealed by a trial-based assay

Márton Kajtor[1], Viktor A. Billes[2,3], Bálint Király[1,4,5], Patricia Karkusova[6], Tibor Kovács[2], Hannah Stabb[1], Katalin Sviatkó[1,7], Andor Vizi[1], Eszter Ujvári[1], Diána Balázsfi[1], Sophie E. Seidenbecher[8], Duda Kvitsiani[9], Tibor Vellai[2,3], Balázs Hangya[1,*]

1 MTA–HUN-REN KOKI Lendület "Momentum" Laboratory of Systems Neuroscience, Institute of Experimental Medicine, H-1083 Budapest, Hungary

2 Department of Genetics, Eötvös Loránd University, H-1117 Budapest, Hungary

3 ELKH-ELTE Genetic Research Group, H-1117 Budapest, Hungary

4 Dynamics of Neural Systems Laboratory, AI Institute, Medical University of Vienna, 1090 Vienna, Austria

5 Department of Biological Physics, Eötvös Loránd University, H-1117 Budapest, Hungary

6 Biomedical Center, Faculty of Medicine in Pilsen, Charles University, 306 05 Pilsen, Czech Republic

7 János Szentágothai Doctoral School of Neurosciences, Semmelweis University, H-1085 Budapest, Hungary

8 University of Technology Nuremberg, Nuremberg, Germany

9 Department of Molecular Biology and Genetics, Danish Research Institute of Translational Neuroscience, Aarhus University, Aarhus, Denmark

* Correspondence: Balázs Hangya, hangya.balazs@koki.hu

## Abstract

The fruit fly *Drosophila melanogaster* emerges as an affordable, genetically tractable model of behavior and brain diseases. However, despite the surprising level of evolutionary conservation from flies to humans, significant genetic, circuit-level and behavioral differences hinder the interpretability of fruit fly models for human disease. Therefore, to allow a more direct fly-versus-human comparison, we surveyed the rarely-exploited, rich behavioral repertoire of fruit flies with genetic alterations relevant to Parkinson's disease (PD). Flies displayed variable behaviors, including freezing, slowing and running, in response to

predator-mimicking passing shadows used as threatening stimuli in a single-animal trial-based assay. We found that the expression of human mutant Parkin in flies resulted in reduced walking speed and decreased reactivity to passing shadows. Flies with dopamine receptor mutations showed similar alterations, consistent with the motor and cognitive deficits typical in humans with PD. We also found age-dependent trends in behavioral choice across the fly lifespan, while dopamine receptor mutant flies maintained their decreased general reactivity throughout all age groups. Our data demonstrate that single-trial behavioral analysis can reveal subtle behavioral changes in mutant flies that can be used to further our understanding of disease pathomechanisms and help gauge the validity of genetic *Drosophila* models of neurodegeneration, taking us one step closer to bridging the gap in fly-to-human translation.

## Introduction

Parkinson's disease (PD) affects over 6 million people worldwide, representing the second most common neurodegenerative disease. PD is slowly progressing and typically leads to years of aggravating disability, thereby placing a huge burden on families, health care systems and the society, measured in hundreds of billions of dollars annually (Olesen et al., 2012; Obeso et al., 2017; Przedborski, 2017; Bloem et al., 2021). Therefore, a hitherto elusive disease-modifying therapy is of prominent priority, envisioned to be fueled by research into basic mechanisms of the disease.

Patients with PD display a diverse set of motor and non-motor symptoms with an underlying progressive loss of midbrain dopaminergic neurons (Schapira, 2009; Schapira et al., 2017; Bloem et al., 2021), mechanisms of which are widely studied in animal models of the disease. Primate models offer the advantage of more direct translatability but are restricted to hard-to-handle neurotoxin approaches and do not promise fast progress. Unlike the genetic mouse models of Alzheimer's disease, most of the successful rodent models of PD are also toxin-based, making it difficult to exploit and further our understanding of the genetic bases of the disease (Cannon and Greenamyre, 2010; Bové and Perier, 2012; Breger and Fuzzati Armentero, 2019). This left a niche for the genetically tractable, affordable fruit flies as genetic models of PD (Feany and Bender, 2000; Guo, 2012; Hewitt and Whitworth, 2017), building on the homologies between the vertebrate basal ganglia and the fruit fly central complex (Strausfeld and Hirth, 2013). However, substantial genetic, anatomical, physiological, and behavioral discrepancies between insects and mammals call for better validation methods of fruit fly models for human disease. Therefore, to provide means for a more direct comparison between flies and mammals, we developed a single-animal trial-based behavioral assay that facilitates fine-grained assessment of phenotypical behavioral changes in fruit flies with mutations relevant to understanding human PD.

Genes linked to familial forms of PD may serve as an ideal basis for genetic disease models. Notably, mutations in the *PARK2* gene, which encodes the Parkin protein involved in maintaining mitochondrial integrity, are associated with autosomal-recessive forms of PD (Guo, 2012). Parkin loss-of-function mutant flies were found to have advanced mitochondrial aging, structural mitochondrial damage and a consequential selective loss of dopaminergic neurons (Cackovic et al., 2018), leading to motor deficits assessed by a climbing assay (Chambers et al., 2013; Cackovic et al., 2018), as well as non-motor PD phenotypes including memory deficits (Julienne et al., 2017). Mutations in the *SNCA* gene of α-Synuclein (α-Syn) are also associated with familiar forms of PD (Polymeropoulos et al., 1997) and α-Syn has been shown to accumulate in Lewy-bodies and Lewy-neurites (Spillantini et al., 1997). α-Syn proteins have been found in the pre-synaptic terminals in humans and mice (Kahle et al., 2000) and are thought to be involved in regulating dopamine (DA) synthesis under physiological conditions by reducing tyrosine hydroxylase activity (Perez et al., 2002). Expression of human α-Syn in flies has been proposed as a genetic model of PD, showing age-dependent loss of dopaminergic neurons and locomotor dysfunction in a climbing assay (Feany and Bender, 2000; Haywood and Staveley, 2006). However, other studies found normal locomotion and dopaminergic cell counts in these flies, casting doubts on the validity of this model (Pesah et al., 2005; Nagoshi, 2018).

Despite the observed homology between mammalian and fruit fly DA systems in motor control and the establishment of *Drosophila* PD models based on human genetic information derived from familial PD patients, the role of *Drosophila* DA receptors in locomotor control is not well characterized. Nevertheless, it has been demonstrated that the D1-like DA receptor mediates ethanol-induced locomotion in the ellipsoid body (Kong et al., 2010). Furthermore, *Dop1R1* has been shown to be involved in turning behavior for goal-directed locomotion (Kottler et al., 2019) and startle-induced negative geotaxis (Sun et al., 2018). To shed light on the possible roles of DA receptors in threat-induced motor behaviors, we tested the behavioral responses of three dopamine receptor (*Dop1R1*, *Dop1R2* and *DopEcR*) insertion mutant lines to predator-mimicking passing shadows and compared them to established fruit fly PD models with partially known locomotor deficits.

We found that flies expressing the R275W mutant allele of human Parkin ('Parkin flies') showed slower average locomotion speed, which, in contrast, was not characteristic of flies expressing the A53T mutant allele of the human *SNCA* gene ('α-Syn flies'). Parkin flies also showed less behavioral reactivity to passing shadows compared to controls, whereas α-Syn flies showed increased durations of stopping after the stimuli. Dopamine receptor mutant flies showed reduced speed and less behavioral reactivity similar to

Parkin flies. *Dop1R1* mutant flies exhibited more pronounced behavioral alterations than the other two receptor mutants in most of the parameters tested. These data demonstrate that mutations in DA receptor genes lead to specific patterns of behavioral deficits in *Drosophila*; hence, these dopamine receptor paralogs may have different functions in behavioral control. The modest phenotype of A53T α-Syn compared to Parkin flies suggests that the latter should be favored as a genetic model of human PD, at least with respect to the motor deficits examined in this study. We further propose that single-trial analyses such as those we present here help us gain a better understanding of the behavioral changes in fruit fly models of PD and are strong tools for validating *Drosophila* models of human diseases.

## Results

### A single-animal trial-based assay to test behavioral responses to predator-mimicking passing shadows

We designed a behavioral apparatus to examine the responses of individual flies to predator-mimicking passing shadows. To do this, we designed a transparent plexiglass arena (Fig. 1a), featuring 13 tunnels (53 mm x 5 mm) for simultaneous tracking of 13 individual flies. The height of the tunnels (1.5 mm) was designed to allow free walking in two dimensions but prevent jumps and flight. To simulate predatory threat, we created passing 'shadows' (Fig. 1a, right; see Methods) with a sliding red screen presented on a 10.1-inch display placed on the top of the arena. A high frame-rate camera was placed under the arena (Fig. 1a, left), allowing us to simultaneously record the movement of the animals and the shadows (Supplementary Movie 1 and 2). All 13 tunnels housed a single fly in each session, enabling the collection of single-animal data from 13 flies in parallel. The locomotion of individual flies was tracked by custom software developed using the Bonsai visual programming environment (Fig. S1, see Methods). We recorded 40-minute-long sessions, consisting of 40 trials of 2-second-long shadow presentations separated by pseudorandom inter-trial-intervals to prevent the animals from learning temporal expectations of the shadow presentations (Fig. 1b).

Fruit flies exhibit a rich behavioral repertoire upon threatening stimuli, including freezing (or stopping) and various escape behaviors such as jumping, slow or fast take-off and running, modulated by walking speed at the time of the threatening stimulus (Zacarias et al., 2018). To study these behaviors, we calculated the speed and acceleration of fruit flies based on the tracked x-y position of their center of mass (Fig. 2a) and aligned these signals to the presentations of the shadow stimuli. To identify separate response types to the threating stimuli, we applied hierarchical clustering on these stimulus-aligned speed

traces (see Methods). This analysis consistently revealed three main stereotypical behavioral responses across flies in addition to the trials where no significant response was evoked (Fig. 2b). Since jumping and flying was not possible in the arena, fruit flies were restricted to choose among freezing, slowing (also observed in (Zacarias et al., 2018)) and running. While this clustering approach was sufficient to reveal response types qualitatively, cluster boundaries were sensitive to genotype-specific differences across groups of flies (Király and Hangya, 2022). Therefore, for rigorous group comparisons, we determined exact definitions of each response type based on fly speed and acceleration (Fig. 2c). Reactions were considered robust if the absolute value of the acceleration reached 200 $mm/s^2$; otherwise, the trial was classified as a 'no reaction' trial. We considered the reaction as a 'stop' if the animal was moving before shadow presentation and its speed decreased to zero in the first second relative to the shadow presentation. If fly speed decreased to a non-zero value, the trial was defined as 'slow down', and if the fly accelerated after the shadow presentation, the trial was classified as 'speed up' (see also Methods).

**Parkinson's model and dopamine receptor mutant fruit flies showed reduced walking speed and decreased reactivity to threatening stimuli**

To generate PD fly models, we expressed the mutant human Parkin (275W) and α-Syn (A53T) coding transgenes (*UAS-Parkin-275W* and *UAS-α-Syn-A53T*, respectively), applying the UAS-Gal4 system (Duffy, 2002). Transgenes were driven by *Ddc-Gal4* inducing the expression of the correspondent human mutant proteins in dopaminergic and serotoninergic fly neurons. Parkin (275W) and α-Syn (A53T) flies were compared to control animals from the same genetic background without mutant transgenes (*Ddc-Gal4* females were crossed with *isogenic* $w^{1118}$ males; the examined F1 generation flies are referred to as *iso* $w^{1118}$; Fig. 3) or mutants overexpressing GFP (Fig. S2). The same level of eye pigmentation and vision of the compared genotypes was achieved by the prior replacement of the *w** mutant X chromosome of the applied *Ddc-Gal4* stock for that of the wild-type. We also used Mi{MIC} random insertion lines for dopamine receptor mutants, namely $y^1$ *w*; Mi{MIC}Dop1R1*$^{MI04437}$ (BDSC 43773), $y^1$ *w*; Mi{MIC}Dop1R2*$^{MI08664}$ (BDSC 51098) (Pimentel et al., 2016; Harbison et al., 2019), and $w^{1118}$*; PBac{PB}DopEcR*$^{c02142}$*/TM6B, Tb*$^1$ (BDSC 10847) (Ishimoto et al., 2013; Petruccelli et al., 2016, 2020), referred to as Dop1R1, Dop1R2 and DopEcR, respectively. The dopamine receptor mutant groups were compared to their parental strains without the mutations ($y^1$ $w^{67c23}$ served as control for *Dop1R1* and *Dop1R2* and $w^{1118}$ for *DopEcR*; Fig. 3).

To test whether mutant flies showed differences in overall locomotion independent of the threatening stimuli, we analyzed average fly speed in the 200 ms time windows before stimulus presentation. We found that Parkin flies showed reduced mean speed compared to controls which expressed the Gal4 driver alone (24.96% reduction, $p = 6.55 \times 10^{-6}$, Mann-Whitney U-test; Fig. 3a, top), while α-Syn flies did not show significant reduction (p = 0.799, Mann–Whitney U-test). We observed similar changes in dopamine receptor mutant flies, where the *Dop1R1* and *DopEcR* defective lines showed a robust mean speed decrease compared to the control groups (*Dop1R1*, 19.68% decrease compared to $y^1\ w^{67c2}$, p = 0.0016; *DopEcR*, 32.97% decrease compared to $w^{1118}$, p = 0.0034; Fig. 3a, bottom), while the *Dop1R2* mutant flies only showed a non-significant speed decrease (21.73% compared to $y^1\ w^{67c23}$, p = 0.1009, Mann–Whitney U-test).

Next, we tested whether mutant flies showed a difference in their reaction to threatening stimuli. We found that PD model flies showed line-specific alterations in their freezing behavior. Parkin flies froze after stimuli less frequently, stopping in 37.72% of trials compared to the 43.48% observed in the *iso* $w^{1118}$ animals (p = 0.0043, Mann Whitney U-test; Fig. 3b, top). However, in the stop trials, they showed normal duration of pauses in locomotion (p = 0.8018 compared to *iso* $w^{1118}$, Mann Whitney U-test; Fig. 3c, top). In contrast, α-Syn flies showed an unchanged stopping frequency when compared to controls (p = 0.0768 compared to *iso* $w^{1118}$, Mann-Whitney U-test), but their stop durations showed a large increase (116.98% increase compared to *iso* $w^{1118}$, $p = 2.18 \times 10^{-11}$, Mann-Whitney U-test). Interestingly, in contrast to PD model flies, dopamine receptor mutant flies did not show significant differences in their freezing behavior relative to controls (stop proportion: *Dop1R1*, p = 0.0631 compared to $y^1\ w^{67c23}$; *Dop1R2*, p = 0.1838 compared to $y^1\ w^{67c23}$; *DopEcR*, p = 0.1445 compared to $w^{1118}$; Mann-Whitney U-test; Fig. 3b, bottom; stop duration: *Dop1R1*, p = 0.893 compared to $y^1\ w^{67c23}$; *Dop1R2*, p = 0.154 compared to $y^1\ w^{67c23}$; *DopEcR*, p = 0.3576 compared to $w^{1118}$; Mann-Whitney U-test; Fig. 3c, bottom).

α-Syn flies showed a reduced aptitude to increase their speed, or 'run', upon encountering threatening stimuli (26.67% decrease compared to *iso* $w^{1118}$, $p = 8.4 \times 10^{-6}$, Mann-Whitney U-test; Fig. 3d, top). Similar results were found in *Dop1R1* (25% decrease compared to $y^1\ w^{67c23}$, p = 0.0122; Mann-Whitney U-test; Fig. 3d, bottom) and *Dop1R2* (41.67% decrease compared to $y^1\ w^{67c23}$, p = 0.0024, Mann-Whitney U-test), but not in *DopEcR* mutant flies (compared to $w^{1118}$, p = 0.6598, Mann-Whitney U-test). Frequency of slowing, i.e., reducing their speed without freezing in a full stop, was moderately decreased in Parkin (14.38% decrease compared to *iso* $w^{1118}$, p = 0.0723, Mann-Whitney U-test; Fig. 3e, top) and *DopEcR* mutant flies (15.28% decrease compared to *iso* $w^{1118}$, p = 0.020, Mann-Whitney U-test; Fig. 3e, bottom).

Overall, all mutations tested resulted in decreased reactivity to threatening stimuli, confirmed by a significant increase in the proportion of trials where no reactions were detected (Fig. 3f). This effect was significant for Parkin flies (30% increase compared to *iso* $w^{1118}$, p = 0.0043, Mann-Whitney U-test), as well as for *Dop1R1* (50% increase compared to $y^1$ $w^{67c23}$, p = 0.0173, Mann-Whitney U-test) and *DopEcR* mutant flies (50% increase compared to *iso* $w^{1118}$, p = 0.0167, Mann-Whitney U-test), but not for α-Syn (α-Syn vs. *iso* $w^{1118}$, p = 0.151, Mann-Whitney U-test) and *Dop1R2* mutant flies (*Dop1R2* vs. $y^1$ $w^{67c23}$, p = 0.1903, Mann-Whitney U-test).

While *Ddc-Gal4* lines are widely used (Wang et al., 2007), they express mutations both in dopaminergic and serotonergic neurons, preventing the assessment of whether the behavioral differences were due to one of those cell types alone. To address this, we tested *NP6510-Gal4-R275W* (Parkin) and *NP6510-Gal4-A53T* (α-Syn) as well as *TH-Gal4-R275W* (Parkin) and *TH-Gal4-A53T* (α-Syn) flies where expression of the mutation was restricted to dopaminergic cells (Riemensperger et al., 2013). Results from these tests were largely similar to those of the *Ddc-Gal4* lines (Fig. S3), reproducing the decreased speed (*NP6510-Gal4-R275W*, 30.3% decrease compared to *NP6510-Gal4- iso* $w^{1118}$, p = 1.55 x $10^{-6}$; *NP6510-Gal4-A53T*, 20.4% decrease compared to *NP6510-Gal4- iso* $w^{1118}$, p = 5.82 x $10^{-10}$; *TH-Gal4-R275W*, 13.08% decrease compared to *TH-Gal4- iso* $w^{1118}$, p = 1.49 x $10^{-6}$; *TH-Gal4-A53T*, 17.57% decrease compared to *TH-Gl4- iso* $w^{1118}$, p = 6.75 x $10^{-7}$; Mann–Whitney U-test) and decreased overall reactivity (*NP6510-Gal4-R275W*, 57.14% increase in 'No reaction' compared to *NP6510-Gal4- iso* $w^{1118}$, p = $3.49^{-8}$; *NP6510-Gal4-A53T*, 14.28% increase in 'No reaction' compared to *NP6510-Gal4- iso* $w^{1118}$, p = 0.1658; *TH-Gal4-R275W*, 66.7% increase in 'No reaction' compared to *TH-Gal4- iso* $w^{1118}$, p = 2.77 x $10^{-10}$; *TH-Gal4-A53T*, 66.7% increase in 'No reaction' compared to *TH-Gal4- iso* $w^{1118}$, p = 1.11 x $10^{-6}$; Mann–Whitney U-test) of PD-model flies. Nevertheless, *TH-Gal4* and *NP6510-Gal4* mutants showed an increased propensity to stop (*NP6510-Gal4-R275W*, 16.47% increase compared to *NP6510-Gal4- iso* $w^{1118}$, p = 4.4 x $10^{-11}$; *NP6510-Gal4-A53T,* 20.17% increase compared to *NP6510-Gal4- iso* $w^{1118}$, p = 1.38 x $10^{-17}$; *TH-Gal4-R275W*, 16.32% increase compared to *TH-Gal4- iso* $w^{1118}$, p = 1.55 x $10^{-4}$; *TH-Gal4-A53T*, 22.41% increase compared to *TH-Gal4- iso* $w^{1118}$, p = 8.82 x $10^{-10}$, Mann–Whitney U-test). Stop duration showed a significant increase not only in α-Syn but also in Parkin fruit flies (*NP6510-Gal4-R275W*, 42.6% increase compared to *NP6510-Gal4- iso* $w^{1118}$, p = $5.99^{-5}$; *NP6510-Gal4-A53T*, 69.5% increase compared to *NP6510-Gal4- iso* $w^{1118}$, p = 4.33 x $10^{-11}$; *TH-Gal4-R275W*, 33.62% increase compared to *TH-Gal4- iso* $w^{1118}$, p = 1.63 x $10^{-6}$; *TH-Gal4-A53T*, 37.48% increase compared to *TH-Gal4- iso* $w^{1118}$, p = 3.89 x $10^{-7}$; Mann–Whitney U-test). Overall, this suggests that mutations in the dopaminergic neurons alone were sufficient to produce the above-described phenotypical changes.

After these detailed comparisons of central tendencies of behavioral data, we also tested whether behavioral variability within fly response types showed differences across mutant groups. We found that stop duration showed a significantly larger dispersion in α-Syn flies compared to controls ($p = 0.0001$, permutation test; Fig. S4), while no other significant difference in data variance was detected.

**Reaction to threatening stimuli depends on fly walking speed**

It has been shown that fruit flies may exhibit a different choice of escape behavior based on their momentary speed when encountering the threat (Zacarias et al., 2018). Therefore, we tested whether mutations in genes relevant to PD caused a change in this speed - behavioral response relationship. We calculated the probability of stopping, slowing, speeding up and no reaction as a function of speed for all mutants, as well as the ratio of each response type conditioned on walking speed at the time of shadow presentations (Fig. 4a-b). These analyses confirmed that 'running' and 'no reaction' was most likely at slow (< 5 mm/s) or zero walking speeds, while slowing down was more frequent as the walking speed increased. Freezing was most frequently observed in the 5-13 mm/s speed range. We did not observe significant difference between groups in their speed - behavioral response relationship for any of the response types (stops, $p = 0.4226$; slow down, $p = 0.6025$; speed up, $p = 0.9074$; no reaction $p = 0.4692$; two-way ANOVA genotype × speed interaction).

Since the distribution of the expression of various escape behaviors depended on walking speed, which was also different across the mutant lines tested (Fig. 3), we asked whether the difference in baseline speed could explain the observed differences in behavioral reactions. Therefore, we performed simulations where reaction probabilities were based on the baseline walking speed distribution of each mutant line to test whether behavioral responses could be predicted based on speed alone (Fig. S5). In most of the groups we found a significant difference between the predicted and the measured response type distributions, suggesting a role for other behavioral differences among the mutant lines beyond the baseline speed differences (Parkin, $p = 0.0487$; α-Syn, $p < 0.000001$; *Dop1R1*, $p = 0.332$; *Dop1R2*, $p = 0.006157$; *DopEcR*, $p = 0.003901$, chi-square test).

**Changes in escape behavior from the first to the fourth week of life**

The age of *Drosophilae* may have a significant influence on their responses to threatening stimuli. To test this, we examined control and dopamine receptor mutant flies ($w^{1118}$, $y^{1}$ $w^{67c23}$, *Dop1R1*, *Dop1R2*, *DopEcR*) in 5 age groups: from 1-day-old to 4-week-old (Fig. 5; Fig. S6). The animals were kept under conditions that accelerated their aging (29°C and 70% humidity). Our data showed that the behavior of 1-day-old flies was significantly different from all other age groups. One-day-old flies stopped significantly more often, and the frequency of stopping gradually decreased with age in all groups (two-way ANOVA, age, $p = 1.87 \times 10^{-20}$, $f = 26.11$; genotype, $p = 1.3 \times 10^{-29}$, $f = 38.42$; genotype × age, $p = 3.18 \times 10^{-6}$, $f = 3.54$; 1-day-old vs. 1-week-old, $p = 1.1 \times 10^{-4}$; 1-week-old vs. 2-week-old, $p = 0.0074$, 2-week-old vs. 3-week-old, $p = 0.1015$; 3-week-old vs. 4-week-old, $p = 0.0079$, Mann-Whitney test for post hoc analysis). In contrast, the probability of slowing down showed a substantial increase from 1-day-old to 1-week-old animals, and then remained relatively stable until the 4th week (two-way ANOVA, age, $p = 9.11 \times 10^{-15}$, $f = 18.72$; genotype, $p = 1.4 \times 10^{-21}$, $f = 27.59$; genotype × age, $p = 0.0028$, $f = 2.291$; 1-day-old vs. 1-week-old, $p = 5.9 \times 10^{-10}$; 1-week-old vs. 2-week-old, $p = 0.992$; 2-week-old vs. 3-week-old, $p = 0.0305$; 3-week-old vs. 4-week-old, $p = 0.033$; Mann-Whitney test for post hoc analysis). The probability of speeding up showed a similar trend, except that the 4-week-old animals showed a significant decrease compared to 3-week-old flies (two-way ANOVA, age, $p = 2.48 \times 10^{-15}$, $f = 19.44$; genotype, $p = 2.28 \times 10^{-44}$, $f = 59.48$; genotype × age, $p = 1.1 \times 10^{-7}$, $f = 4.12$; 1-day-old vs 1-week-old, $p = 2.64 \times 10^{-10}$; 1-week-old vs. 2-week-old, $p = 0.572$; 2-week-old vs. 3-week-old, $p = 0.3445$; 3-week-old vs. 4-week-old, $p = 0.0179$; Mann-Whitney test for post hoc analysis). Thus, different types of escape reactions showed remarkable tendencies across the fly lifespan, while dopamine receptor mutant flies maintained their decreased general reactivity throughout all age groups.

## Discussion

We tested *Drosophila* mutant strains relevant for Parkinson's disease in a single-trial single-animal behavioral assay. Our tests revealed strain-specific behavioral alterations in flies' reactions to predator-mimicking passing shadows, serving as proof of principle demonstration of the viability of single-trial approaches in *Drosophila*, a method widely used in mammalian studies. Specifically, we found reduced walking speed, decreased freezing frequency and decreased overall reactivity in Parkin flies. In contrast, α-Syn flies merely showed an increased freezing duration without a concomitant change in freezing frequency, suggesting that Parkin flies better recapitulate some behavioral features of human PD progression. *Dop1R* mutant flies resembled Parkin flies in their decreased walking speed and decreased

reactivity to the threatening stimuli. The distribution of the behavioral response fruit flies chose to execute depended on their speed at the time of stimuli, and this speed - behavioral response relationship was robust across the tested genotypes. Nevertheless, differences in walking speed alone did not explain the strain-specific behavioral alterations. Age-dependence of behavioral choice was also found to be stereotypic across the tested genotypes.

Recent studies increasingly recognize the importance of investigating subtle changes in fly behavior to better understand the manifestations of locomotor and other disorders (Geissmann et al., 2017; Zacarias et al., 2018; Seidenbecher et al., 2020). Along these lines, Aggarwal and colleagues introduced an automated climbing assay for fruit flies and revealed subtle motor deficits in different mutant strains (Aggarwal et al., 2019). We expanded the scope of these studies by examining a diverse behavioral repertoire of *Drosophila* in response to threatening stimuli. Many earlier studies used looming stimulus, that is, a concentrically expanding shadow, mimicking the approach of a predator from above, to study escape responses in flies (Card and Dickinson, 2008; de Vries and Clandinin, 2012; Zacarias et al., 2018; Ache et al., 2019; Oram and Card, 2022) as well as rodents (Lecca et al., 2017; Braine and Georges, 2023; Heinemans and Moita, 2024). These assays have the advantage of closely resembling naturalistic, ecologically relevant threat-inducing stimuli, and allow a relatively complete characterization of the fly escape behavior repertoire (Zacarias et al., 2018). As a flip side of their large degree of freedom, they do not lend themselves easily to provide a fully standardized, scalable behavioral assay. Therefore, Gibson et al. suggested a novel threat-inducing assay operating with moving overhead translational stimuli, that is, passing shadows, and demonstrated that they induce escape behaviors in flies akin to looming discs (Gibson et al., 2015). This assay, coined ReVSA (repetitive visual stimulus-induced arousal) by the authors, had the advantage of scalability, while constraining flies to a walking arena that somewhat restricted the remarkably rich escape types flies otherwise exhibit. Here we carried this idea one step further by using a screen to present the shadows instead of a physically moving paddle and putting individual flies to linear corridors instead of the common circular fly arena. This ensured that the shadow reached the same coordinates in all linear tracks concurrently and made it easy to accurately determine when individual flies encountered the stimulus, aiding data analysis and scalability. We found the same escape behavioral repertoire as in studies with looming stimuli and ReVSA (Gibson et al., 2015; Zacarias et al., 2018), with a similar dependence on walking speed (Zacarias et al., 2018; Oram and Card, 2022), confirming that looming stimuli and passing shadows can both be considered as threat-inducing visual stimuli.

301 Mutations in the *PARK2* gene lead to impaired ubiquitination and a consequential mitochondrial
302 dysfunction (Guo, 2010, 2012), and early-onset PD in human patients. This led to the widespread use of
303 Parkin flies as a genetic model of PD (Guo, 2010; Chambers et al., 2013; Aggarwal et al., 2019). Of note,
304 flies that lack Parkin display a significant degeneration of dopaminergic neurons (Whitworth et al., 2005).
305 We found similarities between Parkin and *Dop1R* mutant flies in their altered responses to predator-
306 mimicking passing shadows: reduced walking speed and decreased overall reactivity, suggesting that the
307 lack of dopamine action through *Dop1R* may be one of the common pathways underlying motor deficits.
308 This is in line with a recent study demonstrating impaired startle-induced geotaxis and locomotor
309 reactivity in *Dop1R* mutant flies (Sun et al., 2018), similar to what had been shown for Parkin flies
310 (Aggarwal et al., 2019), and a demonstration of dopaminergic control over walking speed (Marquis and
311 Wilson, 2022). In contrast, flies expressing human α-syn showed moderate changes in motor behavior
312 except for a marked prolongation of freezing duration upon threating stimuli. This is in accordance with
313 studies suggesting that α-syn misexpression is not fully penetrant under some conditions (Pesah et al.,
314 2005; Nagoshi, 2018), and calls for the use of other genetic *Drosophila* models, including Parkin flies, in
315 studying the pathophysics of human PD.

316 The dopamine/ecdysteroid receptor *DopEcR* is a G-protein-coupled dual receptor for dopamine and the
317 steroid hormone ecdysone. It has been proposed that the *DopEcR* may serve as an integrative hub for
318 dopamine-mediated actions and stress responses in fruit flies (Petruccelli et al., 2020). We found that
319 *DopEcR* mutant flies showed decreased mean walking speed, decreased probability of slowing down and
320 decreased overall behavioral reactivity in response to predator-mimicking passing shadows. This pattern
321 of alterations was largely similar to those observed in Parkin and *Dop1R* mutant flies, suggesting that the
322 *DopEcR* may convey similar dopamine-mediated functions as *DopR1* at least in those motor aspects tested
323 in the present study. A recent work demonstrated that serotonin also modulates both walking speed and
324 startle response in flies, suggesting a complex neuromodulatory control over *Drosophila* motor behavior
325 (Howard et al., 2019). We recognize a limitation in using PBac{PB}DopEcRc02142 over the TM6B, Tb1
326 balancer chromosome, as the balancer itself may induce behavioral deficits in flies. We consider this
327 unlikely, as the PBac{PB}DopEcRc02142 mutation demonstrates behavioral effects even in heterozygotes
328 (Ishimoto et al., 2013). Additionally, to our knowledge, no studies have reported behavioral deficits in flies
329 carrying the TM6B, Tb1 balancer chromosome over a wild-type chromosome.

330 In humans, degeneration of midbrain dopaminergic neurons has been found as a direct cause of PD
331 symptoms and DA supplementation with its precursor levodopa has been one of the most successful

therapeutic approaches to date. The fruit fly and mammalian DA systems show a number of homologies which are thought to serve as a good basis for *Drosophila* PD models (Feany and Bender, 2000; Hewitt and Whitworth, 2017). Specifically, a deep-running evolutional conservation has been revealed between the arthropod central complex and the vertebrate basal ganglia, where GABAergic and dopaminergic neurons play key roles in motor control in both phylae (Strausfeld and Hirth, 2013). Clusters of fly dopaminergic neurons that project to the ellipsoid body, the fan-shaped body and the lateral accessory lobes are thought to share homologies with the striatum-projecting dopaminergic neurons of the substantia nigra in mammals. Both the fruit fly central complex and vertebrate basal ganglia mediate a range of functions from motor control and sensorimotor integration to action selection and decision making to motivation (Strauss, 2002; Claridge-Chang et al., 2009; Kong et al., 2010) and learning (McCurdy et al., 2021; Zolin et al., 2021; Fisher et al., 2022; Qiao et al., 2022; Taisz and Jefferis, 2022; Yamada et al., 2023). It has been found that fruit flies lacking the DA-synthetizing tyrosine hydroxylase enzyme in the central nervous system show reduced activity and locomotor deficit that worsen with age, and also exhibit marked impairments in associative learning based on both appetitive and aversive reinforcement (Riemensperger et al., 2011). This is in line with mammalian studies emphasizing the role of the dopaminergic nigrostriatal pathway in controlling goal-directed action (Eban-Rothschild et al., 2016), reinforcement learning (Schultz et al., 1997; Lak et al., 2014), and more recently, conveying aversive information (Menegas et al., 2015, 2018). Our findings are consistent with the apparent homologies across fruit fly and mammalian dopaminergic systems and suggest that a more in-depth investigation of specific behavioral changes and underlying dopamine-related dysfunctions may yield translatable results. We also observed age-related changes in motor behavior in response to threatening stimuli, particularly in 4-week-old flies, which may parallel the age-dependent worsening of PD symptoms in humans.

**Acknowledgements**

We thank the Anne Von Phillipsborn lab, DANDRITE, Aarhus University for the kind gift of the DA receptor mutant lines. Most of the *Drosophila* stocks were obtained from the Bloomington Drosophila Stock Center (NIH P40OD018537). We thank the FENS-Kavli Network of Excellence for fruitful discussions. B.H. was supported by the Eotvos Lorand Research Network, the Hungarian Research Network, the Hungarian Brain Research Program NAP3.0 (NAP2022-I-1/2022) and NAP-KOLL-2023-1/2023 grant by the Hungarian Academy of Sciences, the “Lendület” LP2024-8/2024 grant by the Hungarian Academy of Sciences, and the NKFIH K147097 grant of the National Research, Development and Innovation Office. T.V. was

supported by the grants OTKA (Hungarian Scientific Research Fund) K132439 and VEKOP (VEKOP-2.3.2-16-2017-00014), and by the ELKH/MTA-ELTE Genetics Research Group (01062). TK was supported by the OTKA grant (Hungarian Scientific Research Fund) PD 143786, by the University Excellence Fund of Eötvös Loránd University, Budapest, Hungary (EKA_2022/045-P302-1), and by the National Research Excellence Programme STARTING 150612.

**Data and code availability**

All analysis functions are available at https://github.com/hangyabalazs/Drosophila-behavior-analysis. All data are available at https://figshare.com/s/40539ee040a269bf05e5.

## Methods

### Animals

We used 2-weeks-old *Drosophila melanogaster* (both males and females) raised at 24°C and 60% humidity in a natural light-dark cycle for experiments presented in Figures 1-4. For age-group comparisons (Fig.5.), fruit flies aged 1, 7, 14, 21 and 28 days were used. These flies were raised at 29°C and 70% humidity to accelerate aging.

Three sets of mutant groups were used for behavioral comparison. In the first set of animals we used *w*; UAS-Parkin-R275W* (created in the laboratory of Kah-Leong Lim, Neurodegeneration Research Laboratory, National Neuroscience Institute, Singapore)(Wang et al., 2007; Kovács et al., 2017) and *w*; UAS-alpha-Syn-A53T* (BDSC 8148) from the Eotvos Lorand University (Szinyákovics et al., 2023), with $y^1$, $v^1$; *UAS-GFP* (BDSC 35786) and *+; P{Ddc-GAL4.L}4.36* (modified version of BDSC 7009, the original first chromosome $w^{1118}$ has been replaced to $w^+$ in this study) as controls. For the second set of animals we used *Dop1R1*, *Dop1R2* and *DopEcR* mutant flies kindly donated by the Anne Von Phillipsborn lab, DANDRITE, Aarhus University and $y^1$ *w*; Mi{MIC}Dop1R1*$^{MI04437}$ (BDSC 43773), $y^1$ *w*; Mi{MIC}Dop1R2*$^{MI08664}$ (BDSC 51098), and $w^{1118}$; *PBac{PB}DopEcR*$^{c02142}$*/TM6B,* $Tb^1$ (BDSC 10847) with $w^{1118}$ (BDSC 5905) $y^1$ and $y^1$ $w^{67c23}$ (BDSC 6599) as controls from the Bloomington stock center. Table 1. shows the number of recorded flies for the age group comparisons, and Table 2. shows the number of recorded flies for comparing the mutant groups. For the third set of flies we used w[*]; P{w[+mC]=ple-GAL4.F}3 (*TH-Gal4*), Bloomington Drosophila Stock Center: 8848 (Friggi-Grelin et al., 2003), and y[*] w[*]; P{w[+mW.hs]=GawB}NP6510 (*NP6510-Gal4*), Kyoto DGGR: 113956 (Riemensperger et al., 2013; Majcin Dorcikova et al., 2023). Since it was important

392 to ensure that the animals' light perception was not impaired, we replaced the white loss-of-function
393 mutant allele of the transgenic *Gal4* lines with a wild-type allele. As controls, we used transheterozygous
394 +/ *TH-Gal4* and +/ *NP6510-Gal4* strains in all cases.

| | *Dop1R1* | *Dop1R2* | *DopEcR* | $w^{1118}$ | $y^{1}$ $w^{67c23}$ |
|---|---|---|---|---|---|
| 1-day-old | 35 | 36 | 36 | 35 | 41 |
| 1-week-old | 36 | 54 | 36 | 36 | 36 |
| 2-week-old | 36 | 36 | 36 | 36 | 30 |
| 3-week-old | 35 | 35 | 29 | 36 | 36 |
| 4-week-old | 30 | 36 | 34 | 30 | 30 |

395 Table 1. Number of recorded flies for age group comparisons.

| 2-week-old | No. of flies |
|---|---|
| *Dop1R1* | 45 |
| *Dop1R2* | 47 |
| *DopEcR* | 35 |
| $w^{1118}$ | 46 |
| $y^{1}$, $w^{67c23}$ | 40 |
| Parkin (Ddc) | 78 |
| α-Syn (Ddc) | 69 |
| *iso* $w^{1118}$ | 92 |
| *+GFP* | 65 |
| Parkin (NP6510) | 170 |
| α-Syn (NP6510)_ | 181 |
| *+/ NP6510-Gal4* | 176 |
| Parkin (TH) | 322 |
| α-Syn (TH) | 176 |
| *+/ TH-Gal4* | 282 |

396 Table 2. Number of recorded flies for comparing the mutant groups.

397 **Arena**

398 We designed an arena made of four layers of plexiglass and metal that formed 13 tunnels (Fig. 1a). Each
399 tunnel was 52mm x 5mm × 1.5mm, in which individual flies were able to move freely in two dimensions
400 but could not fly. The bottom layer was a standard transparent plexiglass layer. The second layer
401 contained the tunnel walls made of metal to prevent horizontal spread of light. The third layer was the
402 top of the tunnels, made of transparent plexiglass, which could slide above the tunnel. It also contained a
403 small hole on the side, where the flies could be inserted into the tunnel through a pipette. The fourth

404 layer was a metal cover designed with cut-outs that matched the shape and position of the tunnels to
405 prevent flies in the neighboring tunnels from detecting the shadow before it reached their position.

406 **Movement tracking**

407 Flies were tracked by using a FLIR Camera (FLIR Blackfly S USB3 FLIR Systems, Wilsonville, OR, US) placed
408 under the arena (Fig. 1a). The frame rate was set to 100 frames/second to allow the detection of position
409 with high temporal resolution. The recorded images were processed by Bonsai (2.5.2) tracking software
410 (Lopes et al., 2015), using customized Bonsai code. The code extracts each tunnel area separately from
411 the image and detects flies by selecting the biggest and darkest pixel object in the tunnel area in real time.
412 Fly position coordinates were calculated from the centroid. The software stored x-y position coordinates
413 along with their timestamps in csv files, which were later processed in Matlab R2016a (Mathworks, Natick,
414 MA, US).

415 **Predator-mimicking shadow stimuli**

416 A 10.1-inch screen (HannStar HSD101PWW1-A00,) was placed on the top of the arena. The screen
417 presented a yellow background. We implemented 'shadow' stimuli in red color, as these stimuli were
418 suggested to be perceived by fruit flies as dark shadows and also enabled continuous tracking of the
419 animals (Sharkey et al., 2020). The red color screen represented a large enough contrast change to evoke
420 escape behaviors of flies but also provided sufficient brightness to enable continuous motion tracking. A
421 passing shadow stimulus was chosen, as it was affecting all tunnels simultaneously. To mimic an
422 approaching shadow, a red screen slid in from the side, stayed on for 2 seconds, then slid out. The shadow
423 stimuli were separated by pseudorandomized inter-trial intervals with an approximately exponential
424 distribution with a mean of 52.2 seconds, preventing flies from anticipating the next shadow stimulus.

425 **Identification of behavioral response types to the threatening stimuli**

426 Animal speed was calculated as a function of time in a -200 ms to 1000 ms window around each shadow
427 stimulus in 10 ms time bins. These speed functions were normalized by subtracting the average speed in
428 the 200 ms window before the shadow presentation to reveal stimulus induced absolute instantaneous
429 speed changes. Principal component analysis (PCA) was used to reduce dimensionality of the normalized
430 speed functions in the 1 s interval following shadow presentation in a way that the variance between trials
431 is maximally preserved in the low-dimensional representation. Agglomerative hierarchical clustering was
432 performed in the space spanned by the first three principal components to identify trials with distinct
433 characteristic response types.

434 **Behavior detection**

435 After identifying the four most frequently observed animal responses to shadow presentations, we
436 algorithmically defined them based on the speed and acceleration thresholds. First, we examined the
437 speed of the animal in the 200 ms time window before the shadow ($v_{pre}$); stopping/freezing or slowing
438 down was only possible if the fly had been moving, defined by $v_{pre} > 0$ mm/s. Second, we examined the
439 acceleration ($a_{post}$) in the 1 s interval following the shadow using a 100 ms moving average window to
440 characterize the flies' response. Reactions were considered robust if the absolute value of the acceleration
441 reached 200 mm/s$^2$. A trial was characterized as a 'stop' trial, if the average $v_{pre}$ was above 0 mm/s, the
442 fly's first reaction was deceleration, and 0 mm/s speed was reached before accelerating again. If the first
443 reaction was deceleration but 0 mm/s speed was not reached, the trial was classified as a 'slow down'
444 trial. In 'speed up' trials, the first response following the shadow was acceleration. If the absolute value
445 of $a_{post}$ did not reach the 200 mm/s$^2$ threshold during the 1 s interval following the shadow, the trial was
446 labeled as a 'no reaction' trial.

447 **Data analysis and statistics**

448 Data analysis was performed in Matlab R2016a (Mathworks, Natick, MA, US) using custom-written code.
449 Statistical comparison between groups of flies was performed by two-sided Mann-Whitney U-test. Exact
450 p values are reported in the Results section. We performed multi-group comparison in the 'Changes in
451 escape behavior from the first to the fourth week of life' section using two-way ANOVA, as it is reportedly
452 robust to non-normality of the data (Mooi et al., 2018; Knief and Forstmeier, 2021), while there is a lack
453 of a consensual non-parametric alternative. Nevertheless, Kruskal-Wallis tests for the main effect of age
454 showed significant effects in all genotypes in accordance with the ANOVA, confirming the results (Stop
455 frequency, *DopEcR* $p = 0.0007$; *Dop1R1*, $p = 0.004$; *Dop1R2*, $p = 9.94 \times 10^{-5}$; $w^{1118}$, $p = 9.89 \times 10^{-13}$; $y^1\ w^{67}c^{23}$,
456 $p = 2.54 \times 10^{-5}$; Slowing down frequency, *DopEcR*, $p = 0.0421$; *Dop1R1*, $p = 5.77 \times 10^{-6}$; *Dop1R2*, $p = 0.011$;
457 $w^{1118}$, $p = 2.62 \times 10^{-5}$; $y^1\ w^{67c23}$, $p = 0.0382$; Speeding up frequency, *DopEcR*, $p = 0.0003$; *Dop1R1*, $p = 2.06$
458 $\times 10^{-7}$; *Dop1R2*, $p = 2.19 \times 10^{-6}$; $w^{1118}$, $p = 0.0044$; $y^1\ w^{67c23}$, $p = 1.36 \times 10^{-5}$). We used Mann-Whitney U-test
459 for post hoc analyses to maintain consistent use of tests across figures. Since there is no straightforward
460 way of correcting for multiple comparisons in this case, we reported uncorrected p values and suggest
461 considering them at $p = 0.01$, which minimizes type I errors. Nevertheless, Tukey's tests with the 'honest
462 significance' approach yielded similar results. The effect of movement speed on the distribution of
463 behavioral response types was tested using a nested Monte Carlo simulation framework (Fig. S5). This
464 simulation aimed to model how different movement speeds impact the probability distribution of

465 response types, comparing these simulated outcomes to empirical data. This approach allowed us to
466 determine whether observed differences in response distributions were solely due to speed variations
467 across genotypes or if additional behavioral factors contributed to the differences. First, we calculated the
468 probability of each response type at different specific speed values (outer model). These probabilities
469 were derived from the grand average of all trials across each genotype, capturing the overall tendency at
470 various speeds. Second, we simulated behavior of virtual flies (n = 3000 per genotypes, which falls within
471 the same order of magnitude as the number of experimentally recorded trials from different genotypes)
472 by drawing random velocity values from the empirical velocity distribution specific to the given genotype
473 and then randomly selecting a reaction based on the reaction probabilities associated with the drawn
474 velocity (inner model). Finally, we calculated reaction probabilities for the virtual flies and compared them
475 with real data from animals of the same genotype. Differences were statistically tested by Chi-squared
476 test.

477 **Figure Legends**

478 **Fig. 1. Behavioral apparatus and experimental design.**

479 **a,** Top left, schematic of the experimental setup. Top right, schematic of the fly arena. Bottom left,
480 photograph of the experimental setup. Bottom right, a photograph of the fly arena. **b,** Timeline of a
481 session showing the shadow presentations in red over the yellow background.

482 **Fig. 2. Behavioral characterization of the escape behavior repertoire of individual fruit flies.**

483 **a,** Schematic for calculating speed and acceleration based on tracked position coordinates. **b,** Four
484 characteristic escape behaviors categorized by PCA for an example session of a control fly (w1118; from
485 left; stop, slow down, speed up, no reaction). Top, color-coded heatmaps indicating the walking speed of
486 the fly (blue, low speed; yellow, high speed), aligned to shadow presentations (purple line). Bottom,
487 average moving speed triggered on the shadow presentations (purple line). **c,** Threshold-based
488 classification of behavioral responses (from left, stop, slow down, speed up, no reaction). Top, single-trial
489 example for each response type. Time intervals for calculating the average speed before the shadow
490 presentation (purple) as well as the speed and acceleration after the shadow presentation (light green)
491 are marked. Threshold values for each response type are displayed above the graphs. Middle, average
492 walking speed across the trials from all sessions of $w^{1118}$ flies, sorted by the type of behavioral response.
493 Line and errorshade show mean ± SE. Bottom, scatter plots showing minimal (Stop and Slow down trials)

494 or average (Speed up and No reaction trials) post-stimulus speed vs. average pre-stimulus speed,
495 representing the same trials as above.

496 **Fig. 3. Parkinson's model and dopamine receptor mutant fruit flies showed reduced walking speed and**
497 **decreased reactivity to threatening stimuli.**

498 **a**, Distribution of the mean speed measured in the time window [-0.2, 0] seconds relative to shadow
499 presentation for the different mutant groups. Top, Parkin flies showed reduced mean speed compared to
500 controls (Parkin vs. *iso* $w^{1118}$; $p = 6.55 \times 10^{-6}$, Mann–Whitney U-test). Bottom, *Dop1R1* and *DopEcR* mutant
501 flies showed reduced mean speed compared to controls ($y^1w^{67c23}$ and $w^{1118}$ respectively; p = 0.0016, p =
502 0.0034; Mann-Whitney U-test). **b,** Distribution of the proportion of stop trials in different mutant groups.
503 Parkin flies showed a reduced tendency for stopping compared to *iso* $w^{1118}$ (p = 0.0043, Mann Whitney U
504 test). **c,** Distribution of stop duration in different mutant groups. α-Syn flies showed increased stop
505 durations compared to *iso* $w^{1118}$ ($p = 2.18 \times 10^{-11}$, Mann-Whitney U-test). **d,** Distribution of the proportion
506 of speed up trials in different mutant groups. Top, α-Syn flies showed a reduced tendency to speed up
507 compared to their controls ($p = 8.4 \times 10^{-6}$, Mann-Whitney U-test). Bottom, *Dop1R1* and *Dop1R2* mutant
508 flies also showed a significantly reduced tendency to speed up compared to their controls (p = 0.0122 and
509 p = 0.0024, respectively; Mann-Whitney U-test). **e,** Distribution of the proportion of slow down trials in
510 different mutant groups. Bottom, *DopEcR* showed a 15.04% decrease compared to $w^{1118}$ (p = 0.020, Mann-
511 Whitney U-test). **f,** Distribution of the proportion of 'no reaction' trials in different mutant groups. Top,
512 Parkin mutants showed reduced reactivity compared to *iso* $w^{1118}$ controls (p = 0.0043, Mann-Whitney U-
513 test). Bottom, *Dop1R1* and *DopEcR* mutants also showed reduced reactivity compared to $y^1w^{67c23}$ and $w^{1118}$
514 controls, respectively (p = 0.0173 and p = 0.0167, respectively; Mann-Whitney U-test). Box-whisker plots
515 show median, interquartile range and non-outlier range. *, $p < 0.05$; **, $p < 0.01$; ***, $p < 0.001$. Exact
516 genotypes: *iso* $w^{1118}$: *+; +; Ddc-Gal4/+.* Parkin: *+; +; Ddc-Gal4/UAS-Parkin-R275W*. α-Syn: *+; +; Ddc-*
517 *Gal4/UAS-α-Syn-A53T*. $y^1$ $w^{67c23}$: $y^1$ $w^{67c23}$. *Dop1R*: $y^1$ *w*; Mi{MIC}Dop1R1*$^{MI04437}$. *Dop1R2*: $y^1$ *w*;*
518 *Mi{MIC}Dop1R2*$^{MI08664}$. *DopEcR*: $w^{1118}$*; PBac{PB}DopEcR*$^{c02142}$*/TM6B, Tb*$^1$.

519 **Fig. 4. Reaction to threatening stimuli depends on fly walking speed**.

520 **a,** Probability of a given response type as a function of average fly speed before the shadow presentation
521 (200 ms pre-stimulus time window). From left, stop, slow down, speed up and no reaction trials are
522 quantified. Top, Parkin and α-Syn flies. Bottom, *Dop1R1*, *Dop1R2* and *DopEcR* mutant flies. **b,** Proportion
523 of a given response type as a function of average fly speed before the shadow presentation. Top, Parkin

524 and α-Syn flies. Bottom, *Dop1R1*, *Dop1R2* and *DopEcR* mutant flies. Exact genotypes: *iso* $w^{1118}$: *+; +; Ddc-*
525 *Gal4/+.* Parkin: *+; +; Ddc-Gal4/UAS-Parkin-R275W*. α-Syn: *+; +; Ddc-Gal4/UAS-α-Syn-A53T*. $y^1$ $w^{67c23}$: $y^1$
526 $w^{67c23}$. *Dop1R*: $y^1$ *w*; Mi{MIC}Dop1R1*$^{MI04437}$. *Dop1R2*: $y^1$ *w*; Mi{MIC}Dop1R2*$^{MI08664}$. *DopEcR*: $w^{1118}$*;*
527 *PBac{PB}DopEcR*$^{c02142}$*/TM6B,* $Tb^1$.

528 **Fig. 5. Changes in escape behavior from the first to the fourth week of life**

529 Proportion of responses as a function of age for different groups of mutants and controls. From left to
530 right, stop, slow down, speed up and no reaction trials are quantified. Lines and errorshades show mean
531 and standard error. Exact genotypes: *iso* $w^{1118}$: *+; +; Ddc-Gal4/+.* Parkin: *+; +; Ddc-Gal4/UAS-Parkin-*
532 *R275W*. α-Syn: *+; +; Ddc-Gal4/UAS-α-Syn-A53T*. $y^1$ $w^{67c23}$: $y^1$ $w^{67c23}$. *Dop1R*: $y^1$ *w*; Mi{MIC}Dop1R1*$^{MI04437}$.
533 *Dop1R2*: $y^1$ *w*; Mi{MIC}Dop1R2*$^{MI08664}$. *DopEcR*: $w^{1118}$*; PBac{PB}DopEcR*$^{c02142}$*/TM6B,* $Tb^1$.

534 **Supplementary Figure Legends**

535 **Fig. S1. Picture of the arena from the camera view**

536 The 13 tunnels of the arena from the camera view with the tracking lines showing that the animals can
537 move in 2 dimensions. The tracking line color indicates time, with dark blue and red marking the beginning
538 and the end of the tracking, respectively.

539 **Fig. S2. Parkin and α-Syn fly group escape reaction compared to GFP mutant flies**

540 **a**, Distribution of the mean speed measured in the 0.2 second before shadow presentation for Parkin, α-
541 Syn and +GFP mutant groups. Parkin and α-Syn flies showed reduced mean speed compared to +GFP
542 controls (Parkin vs. +GFP, $p = 1.58 \times 10^{-11}$; α-Syn vs. +GFP, $p = 2.85 \times 10^{-4}$; Mann-Whitney U-test). **b,**
543 Distribution of the proportion of stop trials in different mutant groups. Parkin flies showed a reduced
544 tendency for stopping compared to the +GFP group (Parkin vs. +GFP, $p = 7.1 \times 10^{-5}$; α-Syn vs. +GFP, p =
545 0.67; Mann-Whitney U-test). **c,** Distribution of stop duration in different mutant groups. α-Syn flies
546 showed increased stop durations compared to GFP (Parkin vs. +GFP, p = 0.17; α-Syn vs. +GFP, $p = 3.98 \times$
547 $10^{-10}$; Mann-Whitney U-test). **d,** Distribution of the proportion of speed up trials in different mutant
548 groups. Both Parkin and α-Syn flies showed a reduced tendency to speed up compared to +GFP controls
549 (Parkin vs. +GFP, $p = 8.3 \times 10^{-5}$; α-Syn vs. +GFP, $p = 1.96 \times 10^{-12}$; Mann-Whitney U-test). **e**, Distribution of
550 the proportion of slow down trials in different mutant groups. Parkin flies showed a reduced tendency to
551 slow down compared to +GFP controls (Parkin vs. +GFP, p = 0.044; α-Syn vs. +GFP, p = 0.465; Mann-
552 Whitney U-test). **f**, Distribution of the proportion of 'no reaction' trials in different mutant groups. Both
553 Parkin and α-Syn flies showed reduced reactivity compared to +GFP controls (Parkin vs. +GFP, p = 9.4 x

554 $10^{-13}$; α-Syn vs. +GFP, p = 1,3 x $10^{-8}$; Mann-Whitney U-test). *, p < 0.05; **, p < 0.01; ***, p < 0.001. Exact
555 genotypes: *iso* $w^{1118}$: *+; +; Ddc-Gal4/+.* Parkin: *+; +; Ddc-Gal4/UAS-Parkin-R275W*. α-Syn: *+; +; Ddc-*
556 *Gal4/UAS-α-Syn-A53T*.

557 **Fig. S3. Restricting Parkin and α-Syn mutations to dopaminergic neurons**

558 **a,** Distribution of the mean speed measured in the 0.2 second before shadow presentation for Parkin
559 (R275W), α-Syn (A53T) and control (*iso* $w^{1118}$) groups. Top, *NP6510-Gal4* lines; bottom, *TH-Gal4* lines in all
560 panels. *NP6510-Gal4-R275W*, 30.3% decrease compared to *NP6510-Gal4-iso* $w^{1118}$, p = 1.55 x $10^{-6}$;
561 *NP6510-Gal4-A53T*, 20.4% decrease compared to *NP6510-Gal4-iso* $w^{1118}$, p = 5.82 x $10^{-10}$; *TH-Gal4-R275W*,
562 13.08% decrease compared to *TH-Gal4-iso* $w^{1118}$, p = 1.49 x $10^{-6}$; *TH-Gal4-A53T*, 17.57% decrease
563 compared to *TH-Gl4-iso* $w^{1118}$, p = 6.75 x $10^{-7}$; Mann–Whitney U-test. **b,** Distribution of the proportion of
564 stop trials in different mutant groups. *NP6510-Gal4-R275W*, 16.47% increase compared to *NP6510-Gal4-*
565 *iso* $w^{1118}$, p = 4.4 x $10^{-11}$; *NP6510-Gal4-A53T,* 20.17% increase compared to *NP6510-Gal4-iso* $w^{1118}$, p = 1.38
566 x $10^{-17}$; *TH-Gal4-R275W*, 16.32% increase compared to *TH-Gal4-iso* $w^{1118}$, p = 1.55 x $10^{-4}$; *TH-Gal4-A53T*,
567 22.41% increase compared to *TH-Gal4-iso* $w^{1118}$, p = 8.82 x $10^{-10}$, Mann–Whitney U-test. **c,** Distribution of
568 stop duration in different mutant groups. *NP6510-Gal4-R275W*, 42.6% increase compared to *NP6510-*
569 *Gal4-iso* $w^{1118}$, p = $5.99^{-5}$; *NP6510-Gal4-A53T*, 69.5% increase compared to *NP6510-Gal4-iso* $w^{1118}$, p = 4.33
570 x $10^{-11}$; *TH-Gal4-R275W*, 33.62% increase compared to *TH-Gal4-iso* $w^{1118}$, p = 1.63 x $10^{-6}$; *TH-Gal4-A53T*,
571 37.48% increase compared to *TH-Gal4-iso* $w^{1118}$, p = 3.89 x $10^{-7}$; Mann–Whitney U-test. **d,** Distribution of
572 the proportion of speed up trials in different mutant groups. *NP6510-Gal4-R275W*, 9.1% decrease
573 compared to *NP6510-Gal4-iso* $w^{1118}$, p = 0.0052; *NP6510-Gal4-A53T*, 9.1% decrease compared to *NP6510-*
574 *Gal4-iso* $w^{1118}$, p = 3.14 x $10^{-4}$; *TH-Gal4-R275W*, 13.3% decrease compared to *TH-Gal4-iso* $w^{1118}$, p = 1.25 x
575 $10^{-9}$; *TH-Gal4-A53T*, 20% decrease compared to *TH-Gal4-iso* $w^{1118}$, p = 1.33 x $10^{-15}$; Mann–Whitney U-test.
576 **e,** Distribution of the proportion of slow down trials in different mutant groups. *NP6510-Gal4-R275W*,
577 22.2% decrease compared to *NP6510-Gal4-iso* $w^{1118}$, p = $8.23^{-5}$; *NP6510-Gal4-A53T*, 39.1% decrease
578 *NP6510-Gal4-iso* $w^{1118}$, p = 2.42 x $10^{-10}$; *TH-Gal4-R275W*, 22.8% decrease compared to *TH-Gal4-iso* $w^{1118}$,
579 p = 2.85 x $10^{-8}$; *TH-Gal4-A53T*, 31.49% decrease compared to *TH-Gal4-iso* $w^{1118}$, p = 1.95 x $10^{-11}$; Mann–
580 Whitney U-test. **f,** Distribution of the proportion of 'no reaction' trials in different mutant groups. *NP6510-*
581 *Gal4-R275W*, 57.14% increase compared to *NP6510-Gal4-iso* $w^{1118}$, p = $3.49^{-8}$; *NP6510-Gal4-A53T*, 14.28%
582 increase compared to *NP6510-Gal4-iso* $w^{1118}$, p = 0.1658; *TH-Gal4-R275W*, 66.7% increase compared to
583 *TH-Gal4-iso* $w^{1118}$, p = 2.77 x $10^{-10}$; *TH-Gal4-A53T*, 66.7% increase compared to *TH-Gal4-iso* $w^{1118}$, p = 1.11
584 x $10^{-6}$; Mann–Whitney U-test.

585 **Fig. S4. Stop duration showed large variance in α-Syn flies**

586 **a,** Distributions of stop duration in *iso* $w^{1118}$ controls, Parkin and α-Syn flies. **b,** Permutation tests revealed
587 a significantly increased variance in α-Syn compared to control flies (p = 0.0001). Histograms show
588 shuffled variance difference between Parkin (left) or α-Syn (right) and control groups. Observed difference
589 in variance is indicated by a blue vertical line. The critical value corresponding to p = 0.05 is indicated by
590 a green dashed vertical line.

591 **Fig. S5. Differences in walking speed do not explain different escape behaviors**

592 Real and simulated proportion of response types are shown for the mutant groups tested. For the
593 simulations, random velocity values were drawn from the velocity distribution of each genotype and then
594 a response type was randomly selected based on the response type distributions associated with the
595 drawn velocity. Bar plots show the proportion of response types color-coded. For each mutant group, the
596 right bar shows the measured proportion of escape responses, while the left bar shows the simulated
597 distribution. We found significant differences between the real and simulated distributions for the
598 following groups: Parkin (p = 0.0487), α-Syn (p < 0.000001), *Dop1R2* (p = 0.006157) and *DopEcR* (p =
599 0.003901). We found no significant differences for the *Dop1R1* group (p = 0.332; Chi-square test for all
600 the statistics). *, p < 0.05; **, p < 0.01; ***, p < 0.001. Exact genotypes: *iso* $w^{1118}$: *+; +; Ddc-Gal4/+.* Parkin:
601 *+; +; Ddc-Gal4/UAS-Parkin-R275W*. α-Syn: *+; +; Ddc-Gal4/UAS-α-Syn-A53T*. $y^1$ $w^{67c23}$: $y^1$ $w^{67c23}$. *Dop1R*: $y^1$
602 *w*; Mi{MIC}Dop1R1*$^{MI04437}$. *Dop1R2*: $y^1$ *w*; Mi{MIC}Dop1R2*$^{MI08664}$. *DopEcR*: $w^{1118}$;
603 *PBac{PB}DopEcR*$^{c02142}$*/TM6B, Tb*$^1$.

604 **Fig. S6. Changes in escape behavior from the first to the fourth week of life**

605 **a,** Average walking speed as a function of age for different groups of controls (left) and mutants (right).
606 Lines and errorshades show mean and standard error. Mean speed showed significant differences among
607 age groups (two-way ANOVA, age, f = 41.38, p = 9.39 x $10^{-32}$; genotype, f = 42.19, p = 2.46 x $10^{-32}$; genotype
608 × age, f = 4.36, p = 2.667 x $10^{-8}$;Tukey's post hoc test: 1 day old vs. 1 week old, p = 9.92 x $10^{-9}$; 1 week old
609 vs. 2 weeks old, p = 7.34 x $10^{-7}$; 2 weeks old vs. 3 weeks old, p = 0.085; 3 weeks old vs. 4 weeks old, p =
610 0.0043). **b,** Stop duration as a function of age for different groups of controls (left) and mutants (right).
611 We found that age did not effect the duration of stops (two-way ANOVA, age, f = 0.85, p = 0.49; genotype,
612 f = 0.91, p = 0.46; genotype × age, f = 2.53, p = 0.0008; Tukey's post hoc test: 1 day old vs. 1 week old, p =
613 0.98; 1 week old vs. 2 weeks old, p = 0.992; 2 weeks old vs. 3 weeks old, p = 0.578; 3 weeks old vs. 4 weeks
614 old, p = 0.9759). Lines and errorshades show mean and standard error.

615 **Supplementary Movie 1**

616 Example recording of *iso* $w^{1118}$ files in the arena. Flies could walk freely inside the tunnels, speed up, slow
617 down, stop, turn, climb the side walls, flip, or groom their wings.

618 **Supplementary Movie 2**

619 Example recording of Parkin flies in the arena. Similar behaviors can be observed as in *iso* $w^{1118}$ flies (see
620 Supplementary Movie 1).

621

622 **References**


623 Ache JM, Polsky J, Alghailani S, Parekh R, Breads P, Peek MY, Bock DD, von Reyn CR, Card GM (2019)
624 Neural Basis for Looming Size and Velocity Encoding in the Drosophila Giant Fiber Escape Pathway.
625 Curr Biol 29:1073-1081.e4.

626 Aggarwal A, Reichert H, VijayRaghavan K (2019) A locomotor assay reveals deficits in heterozygous
627 Parkinson's disease model and proprioceptive mutants in adult Drosophila. Proc Natl Acad Sci U S A
628 116:24830–24839.

629 Bloem BR, Okun MS, Klein C (2021) Parkinson's disease. Lancet 397:2284–2303.

630 Bové J, Perier C (2012) Neurotoxin-based models of Parkinson's disease. Neuroscience 211:51–76.

631 Braine A, Georges F (2023) Emotion in action: When emotions meet motor circuits. Neurosci Biobehav
632 Rev 155:105475.

633 Breger LS, Fuzzati Armentero MT (2019) Genetically engineered animal models of Parkinson's disease:
634 From worm to rodent. Eur J Neurosci 49:533–560.

635 Cackovic J, Gutierrez-Luke S, Call GB, Juba A, O'Brien S, Jun CH, Buhlman LM (2018) Vulnerable parkin
636 loss-of-function Drosophila dopaminergic neurons have advanced mitochondrial aging,
637 mitochondrial network loss and transiently reduced autophagosome recruitment. Front Cell
638 Neurosci 12:1–14.

639 Cannon JR, Greenamyre JT (2010) Neurotoxic in vivo models of Parkinson's disease. In: Progress in Brain
640 Research, pp 17–33. Elsevier B.V.

641 Card G, Dickinson MH (2008) Visually Mediated Motor Planning in the Escape Response of Drosophila.
642 Curr Biol 18:1300–1307.

643 Chambers RP, Call GB, Meyer D, Smith J, Techau JA, Pearman K, Buhlman LM (2013) Nicotine increases
644 lifespan and rescues olfactory and motor deficits in a Drosophila model of Parkinson's disease.
645 Behav Brain Res 253:95–102.

646 Claridge-Chang A, Roorda RD, Vrontou E, Sjulson L, Li H, Hirsh J, Miesenböck G (2009) Writing Memories
647 with Light-Addressable Reinforcement Circuitry. Cell 139:405–415.

648 de Vries SEJ, Clandinin TR (2012) Loom-Sensitive Neurons Link Computation to Action in the Drosophila
649 Visual System. Curr Biol 22:353–362.

650 Duffy JB (2002) GAL4 system indrosophila: A fly geneticist's swiss army knife. genesis 34:1–15.

651 Eban-Rothschild A, Rothschild G, Giardino WJ, Jones JR, De Lecea L (2016) VTA dopaminergic neurons
652 regulate ethologically relevant sleep-wake behaviors. Nat Neurosci 19:1356–1366.

653 Feany MB, Bender WW (2000) A Drosophila model of Parkinson's disease. Nature 404:394–398.

654 Fisher YE, Marquis M, D'Alessandro I, Wilson RI (2022) Dopamine promotes head direction plasticity
655 during orienting movements. Nature 612:316–322.

656 Friggi-Grelin F, Coulom H, Meller M, Gomez D, Hirsh J, Birman S (2003) Targeted gene expression in
657 Drosophila dopaminergic cells using regulatory sequences from tyrosine hydroxylase. J Neurobiol
658 54:618–627.

659 Geissmann Q, Garcia Rodriguez L, Beckwith EJ, French AS, Jamasb AR, Gilestro GF (2017) Ethoscopes: An
660 open platform for high-throughput ethomics. PLOS Biol 15:e2003026.

661 Gibson WT, Gonzalez CR, Fernandez C, Ramasamy L, Tabachnik T, Du RR, Felsen PD, Maire MR, Perona P,
662 Anderson DJ (2015) Behavioral Responses to a Repetitive Visual Threat Stimulus Express a
663 Persistent State of Defensive Arousal in Drosophila. Curr Biol 25:1401–1415.

664 Guo M (2010) What have we learned from Drosophila models of Parkinson's disease? In: Progress in
665 Brain Research, pp 2–16. Elsevier B.V.

666 Guo M (2012) Drosophila as a model to study mitochondrial dysfunction in Parkinson's disease. Cold
667 Spring Harb Perspect Med 2:1–18.

668 Harbison ST, Kumar S, Huang W, McCoy LJ, Smith KR, Mackay TFC (2019) Genome-Wide Association
669 Study of Circadian Behavior in Drosophila melanogaster. Behav Genet 49:60–82.

670 Haywood AFM, Staveley BE (2006) Mutant α-synuclein-induced degeneration is reduced by parkin in a
671 fly model of Parkinson's disease. Genome 49:505–510.

672 Heinemans M, Moita MA (2024) Looming stimuli reliably drive innate defensive responses in male rats,
673 but not learned defensive responses. Sci Rep 14:21578.

674 Hewitt VL, Whitworth AJ (2017) Mechanisms of Parkinson's Disease. In: Current Topics in Developmental
675 Biology, 1st ed., pp 173–200. Elsevier Inc.

676 Howard CE, Chen C-L, Tabachnik T, Hormigo R, Ramdya P, Mann RS (2019) Serotonergic Modulation of
677 Walking in Drosophila. Curr Biol 29:4218-4230.e8.

678 Ishimoto H, Wang Z, Rao Y, Wu C, Kitamoto T (2013) A Novel Role for Ecdysone in Drosophila
679 Conditioned Behavior: Linking GPCR-Mediated Non-canonical Steroid Action to cAMP Signaling in
680 the Adult Brain Stern DL, ed. PLoS Genet 9:e1003843.

681 Julienne H, Buhl E, Leslie DS, Hodge JJL (2017) Drosophila PINK1 and parkin loss-of-function mutants
682 display a range of non-motor Parkinson's disease phenotypes. Neurobiol Dis 104:15–23.

683 Kahle PJ, Neumann M, Ozmen L, Müller V, Jacobsen H, Schindzielorz A, Okochi M, Leimer U, Van Der
684 Putten H, Probst A, Kremmer E, Kretzschmar HA, Haass C (2000) Subcellular localization of wild-
685 type and Parkinson's disease-associated mutant α-synuclein in human and transgenic mouse brain.
686 J Neurosci 20:6365–6373.

687 Király B, Hangya B (2022) Navigating the Statistical Minefield of Model Selection and Clustering in
688 Neuroscience. eNeuro 9.

689 Knief U, Forstmeier W (2021) Violating the normality assumption may be the lesser of two evils. Behav
690 Res Methods 53:2576–2590.

691 Kong EC, Woo K, Li H, Lebestky T, Mayer N, Sniffen MR, Heberlein U, Bainton RJ, Hirsh J, Wolf FW (2010)
692 A pair of dopamine neurons target the D1-like dopamine receptor dopr in the central complex to
693 promote ethanol-stimulated locomotion in drosophila. PLoS One 5.

694 Kottler B, Faville R, Bridi JC, Hirth F (2019) Inverse Control of Turning Behavior by Dopamine D1 Receptor
695 Signaling in Columnar and Ring Neurons of the Central Complex in Drosophila. Curr Biol 29:567-

577.e6.

Kovács T et al. (2017) The small molecule AUTEN-99 (autophagy enhancer-99) prevents the progression of neurodegenerative symptoms. Sci Rep 7:42014.

Lak A, Stauffer WR, Schultz W (2014) Dopamine prediction error responses integrate subjective value from different reward dimensions. Proc Natl Acad Sci U S A 111:2343–2348.

Lecca S, Meye FJ, Trusel M, Tchenio A, Harris J, Schwarz MK, Burdakov D, Georges F, Mameli M (2017) Aversive stimuli drive hypothalamus-to-habenula excitation to promote escape behavior. Elife 6:1–16.

Lopes G, Bonacchi N, Frazão J, Neto JP, Atallah B V., Soares S, Moreira L, Matias S, Itskov PM, Correia PA, Medina RE, Calcaterra L, Dreosti E, Paton JJ, Kampff AR (2015) Bonsai: an event-based framework for processing and controlling data streams. Front Neuroinform 9:7.

Majcin Dorcikova M, Duret LC, Pottié E, Nagoshi E (2023) Circadian clock disruption promotes the degeneration of dopaminergic neurons in male Drosophila. Nat Commun 14:5908.

Marquis M, Wilson RI (2022) Locomotor and olfactory responses in dopamine neurons of the Drosophila superior-lateral brain. Curr Biol 32:5406-5414.e5.

McCurdy LY, Sareen P, Davoudian PA, Nitabach MN (2021) Dopaminergic mechanism underlying reward-encoding of punishment omission during reversal learning in Drosophila. Nat Commun 12:1115.

Menegas W, Akiti K, Amo R, Uchida N, Watabe-Uchida M (2018) Dopamine neurons projecting to the posterior striatum reinforce avoidance of threatening stimuli. Nat Neurosci 21:1421–1430.

Menegas W, Bergan JF, Ogawa SK, Isogai Y, Venkataraju KU, Osten P, Uchida N, Watabe-Uchida M (2015) Dopamine neurons projecting to the posterior striatum form an anatomically distinct subclass. Elife 4:1–30.

Mooi E, Sarstedt M, Mooi-Reci I (2018) Market Research. Singapore: Springer Singapore.

Nagoshi E (2018) Drosophila Models of Sporadic Parkinson's Disease. Int J Mol Sci 19:3343.

Obeso JA et al. (2017) Past, present, and future of Parkinson's disease: A special essay on the 200th Anniversary of the Shaking Palsy. Mov Disord 32:1264–1310.

Olesen J, Gustavsson a., Svensson M, Wittchen HU, Jönsson B (2012) The economic cost of brain

723 disorders in Europe. Eur J Neurol 19:155–162.

724 Oram TB, Card GM (2022) Context-dependent control of behavior in Drosophila. Curr Opin Neurobiol
725 73:102523.

726 Perez RG, Waymire JC, Lin E, Liu JJ, Guo F, Zigmond MJ (2002) A Role for α-Synuclein in the Regulation of
727 Dopamine Biosynthesis. J Neurosci 22:3090–3099.

728 Pesah Y, Burgess H, Middlebrooks B, Ronningen K, Prosser J, Tirunagaru V, Zysk J, Mardon G (2005)
729 Whole-mount analysis reveals normal numbers of dopaminergic neurons following misexpression
730 of?-Synuclein inDrosophila. genesis 41:154–159.

731 Petruccelli E, Lark A, Mrkvicka JA, Kitamoto T (2020) Significance of DopEcR, a G-protein coupled
732 dopamine/ecdysteroid receptor, in physiological and behavioral response to stressors. J
733 Neurogenet 34:55–68.

734 Petruccelli E, Li Q, Rao Y, Kitamoto T (2016) The Unique Dopamine/Ecdysteroid Receptor Modulates
735 Ethanol-Induced Sedation in Drosophila. J Neurosci 36:4647–4657.

736 Pimentel D, Donlea JM, Talbot CB, Song SM, Thurston AJF, Miesenböck G (2016) Operation of a
737 homeostatic sleep switch. Nature 536:333–337.

738 Polymeropoulos MH et al. (1997) Mutation in the α-synuclein gene identified in families with Parkinson's
739 disease. Science (80- ) 276:2045–2047.

740 Przedborski S (2017) The two-century journey of Parkinson disease research. Nat Rev Neurosci 18:251–
741 259.

742 Qiao J, Yang S, Geng H, Yung W-H, Ke Y (2022) Input-timing-dependent plasticity at incoming synapses of
743 the mushroom body facilitates olfactory learning in Drosophila. Curr Biol 32:4869-4880.e4.

744 Riemensperger T, Isabel G, Coulom H, Neuser K, Seugnet L, Kume K, Iché-Torres M, Cassar M, Strauss R,
745 Preat T, Hirsh J, Birman S (2011) Behavioral consequences of dopamine deficiency in the
746 Drosophila central nervous system. Proc Natl Acad Sci U S A 108:834–839.

747 Riemensperger T, Issa A-R, Pech U, Coulom H, Nguyễn M-V, Cassar M, Jacquet M, Fiala A, Birman S
748 (2013) A Single Dopamine Pathway Underlies Progressive Locomotor Deficits in a Drosophila Model
749 of Parkinson Disease. Cell Rep 5:952–960.

750 Schapira AHV (2009) Neurobiology and treatment of Parkinson's disease. Trends Pharmacol Sci 30:41–
751 47.

752 Schapira AHV, Chaudhuri KR, Jenner P (2017) Non-motor features of Parkinson disease. Nat Rev
753 Neurosci 18:435–450.

754 Schultz W, Dayan P, Montague PR (1997) A neural substrate of prediction and reward. Science
755 275:1593–1599.

756 Seidenbecher SE, Sanders JI, von Philipsborn AC, Kvitsiani D (2020) Reward foraging task and model-
757 based analysis reveal how fruit flies learn value of available options Skoulakis EMC, ed. PLoS One
758 15:e0239616.

759 Sharkey CR, Blanco J, Leibowitz MM, Pinto-Benito D, Wardill TJ (2020) The spectral sensitivity of
760 Drosophila photoreceptors. Sci Rep.

761 Spillantini MG, Schmidt ML, Lee VM-Y, Trojanowski JQ, Jakes R, Goedert M (1997) α-Synuclein in Lewy
762 bodies. Nature 388:839–840.

763 Strausfeld NJ, Hirth F (2013) Deep homology of arthropod central complex and vertebrate basal ganglia.
764 Science (80- ) 340:157–161.

765 Strauss R (2002) The central complex and the genetic dissection of locomotor behaviour. Curr Opin
766 Neurobiol 12:633–638.

767 Sun J, Xu AQ, Giraud J, Poppinga H, Riemensperger T, Fiala A, Birman S (2018) Neural control of startle-
768 induced locomotion by the mushroom bodies and associated neurons in drosophila. Front Syst
769 Neurosci 12:1–18.

770 Szinyákovics J, Keresztes F, Kiss EA, Falcsik G, Vellai T, Kovács T (2023) Potent New Targets for Autophagy
771 Enhancement to Delay Neuronal Ageing. Cells 12:1753.

772 Taisz I, Jefferis GSXE (2022) Speed of learning depends on turning. Nature 612:216–217.

773 Wang C, Lu R, Ouyang X, Ho MWL, Chia W, Yu F, Lim K-L (2007) Drosophila Overexpressing Parkin R275W
774 Mutant Exhibits Dopaminergic Neuron Degeneration and Mitochondrial Abnormalities. J Neurosci
775 27:8563–8570.

776 Whitworth AJ, Theodore DA, Greene JC, Beneš H, Wes PD, Pallanck LJ (2005) Increased glutathione S -

transferase activity rescues dopaminergic neuron loss in a Drosophila model of Parkinson's disease. Proc Natl Acad Sci 102:8024–8029.

Yamada D, Bushey D, Li F, Hibbard KL, Sammons M, Funke J, Litwin-Kumar A, Hige T, Aso Y (2023) Hierarchical architecture of dopaminergic circuits enables second-order conditioning in Drosophila. Elife 12:1–30.

Zacarias R, Namiki S, Card GM, Vasconcelos ML, Moita MA (2018) Speed dependent descending control of freezing behavior in Drosophila melanogaster. Nat Commun 9:1–11.

Zolin A, Cohn R, Pang R, Siliciano AF, Fairhall AL, Ruta V (2021) Context-dependent representations of movement in Drosophila dopaminergic reinforcement pathways. Nat Neurosci 24:1555–1566.

**Figures**

**Figure 1**

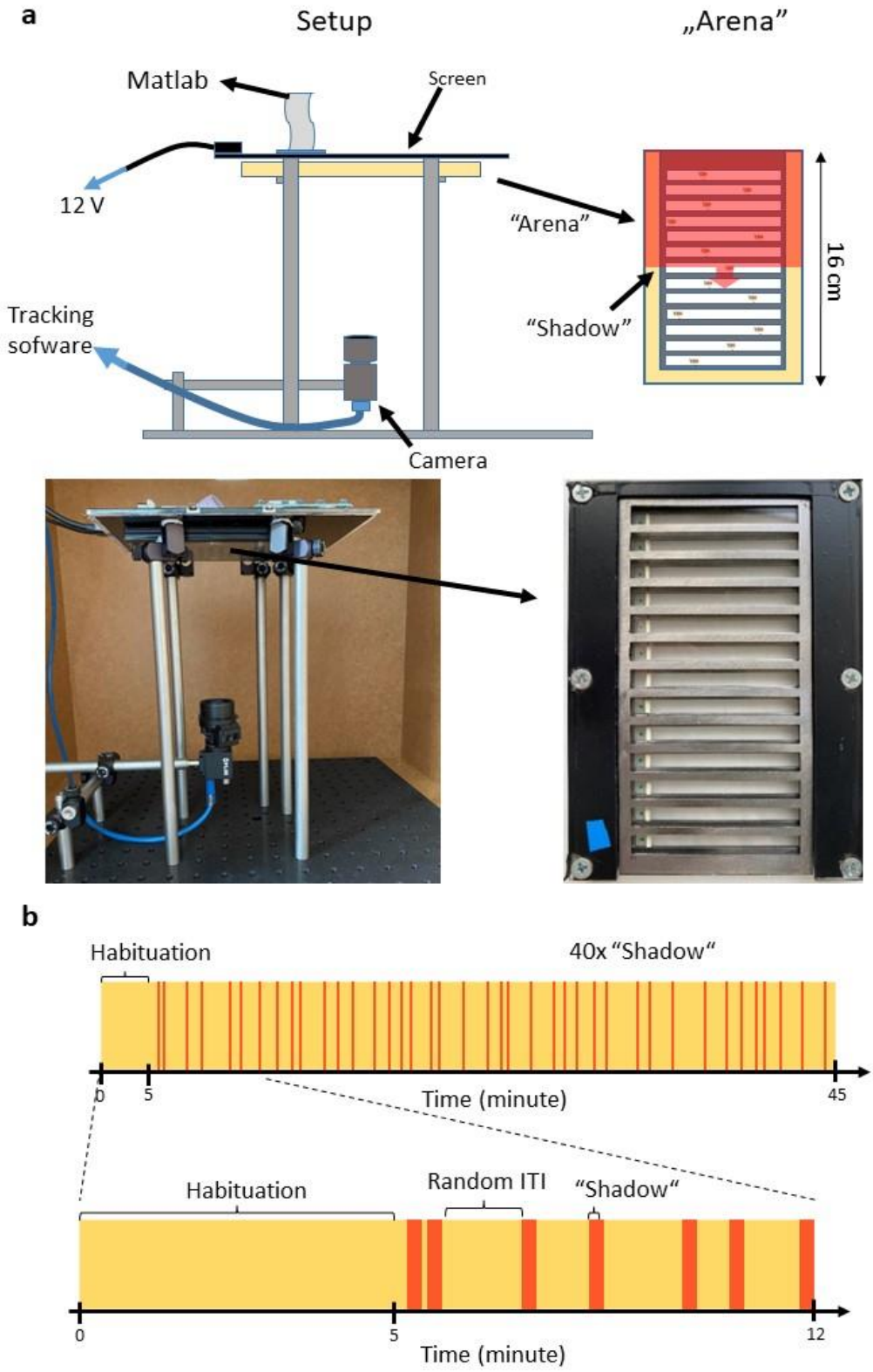

**Figure 2**

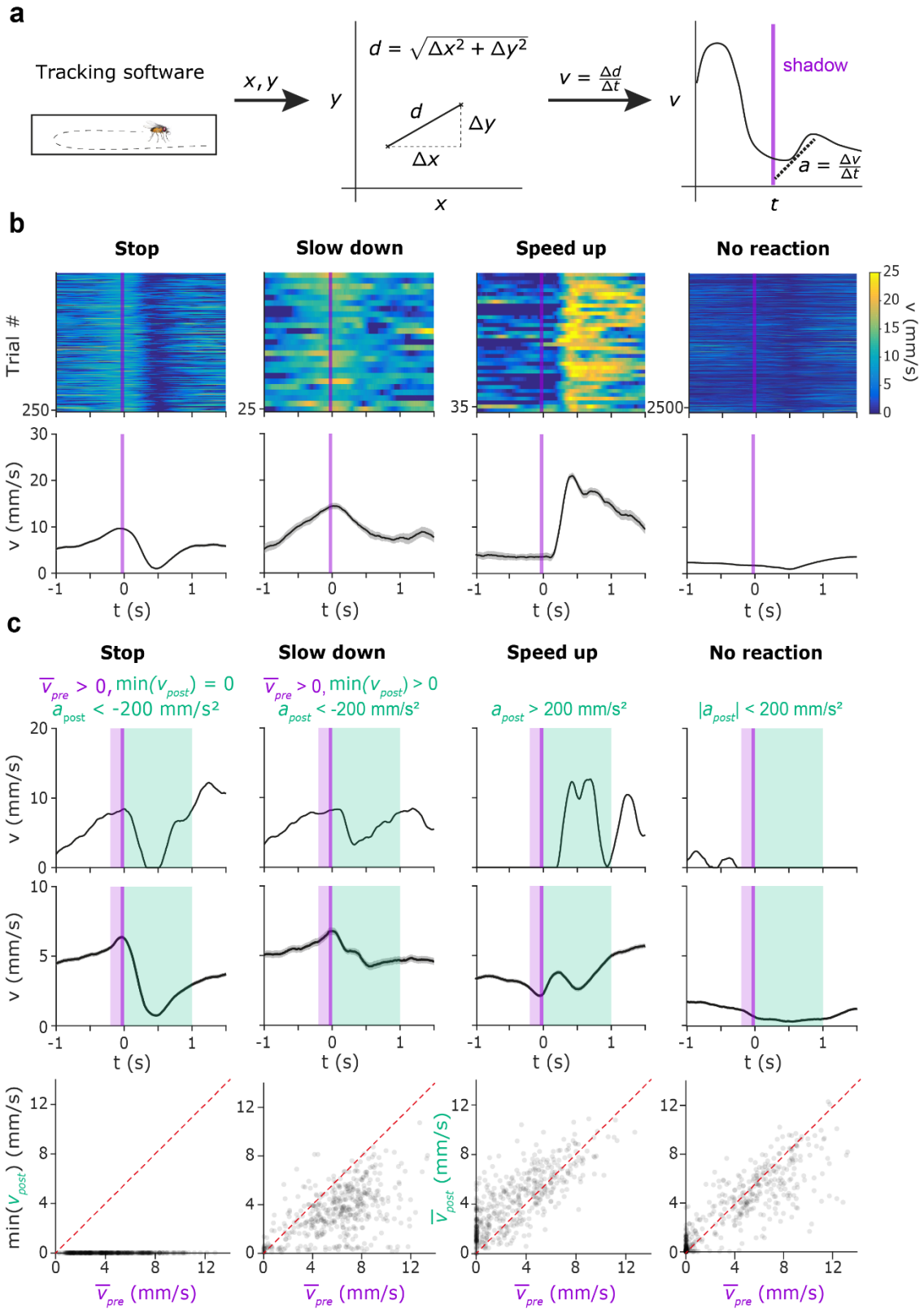
a
Tracking software
x, y
y
x
d = √(Δx² + Δy²)
d
Δy
Δx
v = Δd/Δt
v
t
shadow
a = Δv/Δt
b
Stop
Slow down
Speed up
No reaction
Trial #
250
25
35
2500
v (mm/s)
t (s)
c
Stop
Slow down
Speed up
No reaction
v̄pre > 0, min(vpost) = 0
apost < -200 mm/s²
v̄pre > 0, min(vpost) > 0
apost < -200 mm/s²
apost > 200 mm/s²
|apost| < 200 mm/s²
min(vpost) (mm/s)
v̄post (mm/s)
v̄pre (mm/s)

**Figure 3**

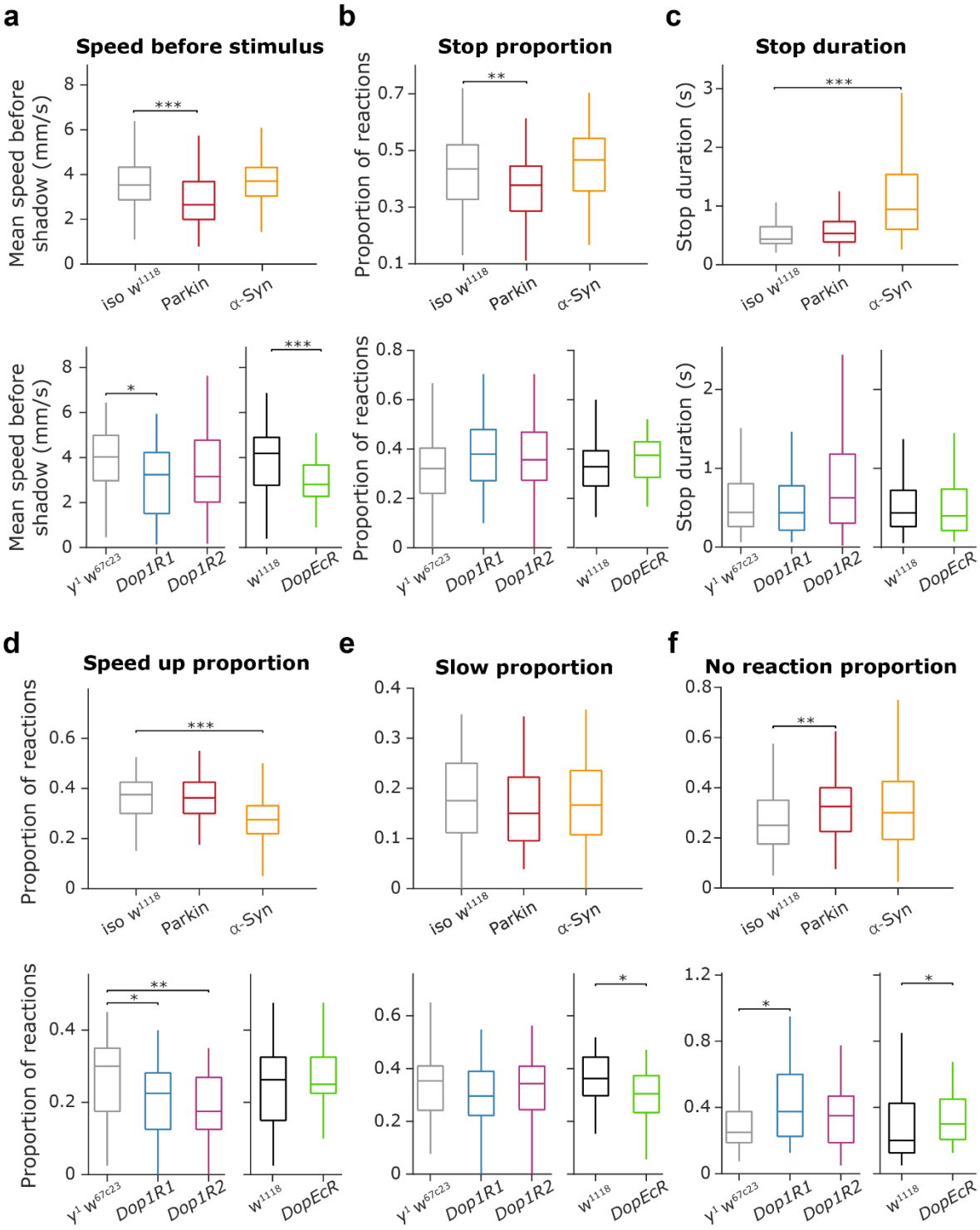
a
Speed before stimulus
Mean speed before shadow (mm/s)
iso w1118
Parkin
α-Syn
y1 w67c23
Dop1R1
Dop1R2
w1118
DopEcR
b
Stop proportion
Proportion of reactions
c
Stop duration
Stop duration (s)
d
Speed up proportion
e
Slow proportion
f
No reaction proportion

**Figure 4**

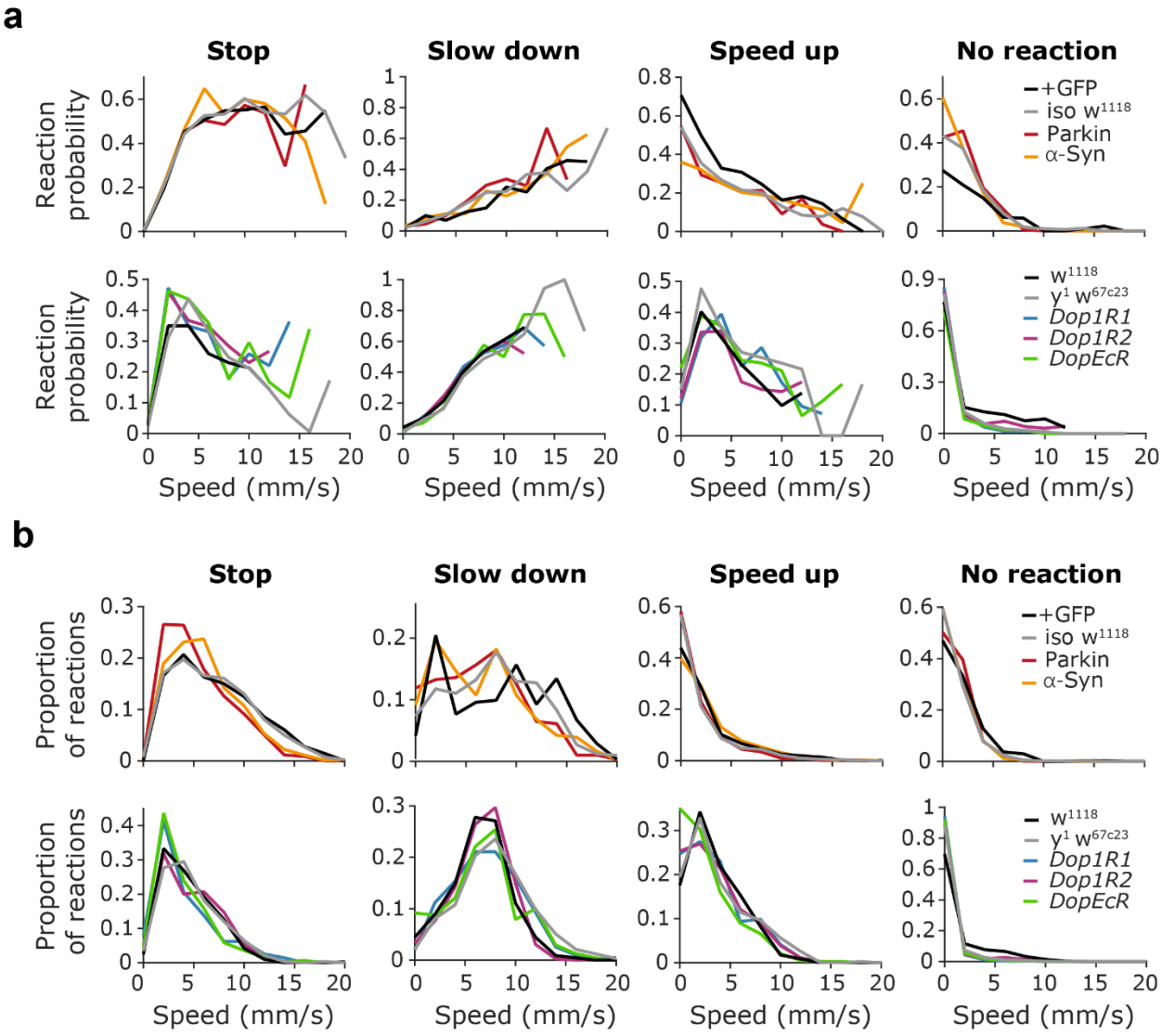
a
Stop
Slow down
Speed up
No reaction
Reaction probability
+GFP
iso w1118
Parkin
α-Syn
w1118
y1 w67c23
Dop1R1
Dop1R2
DopEcR
Speed (mm/s)
b
Proportion of reactions

800 **Figure 5**

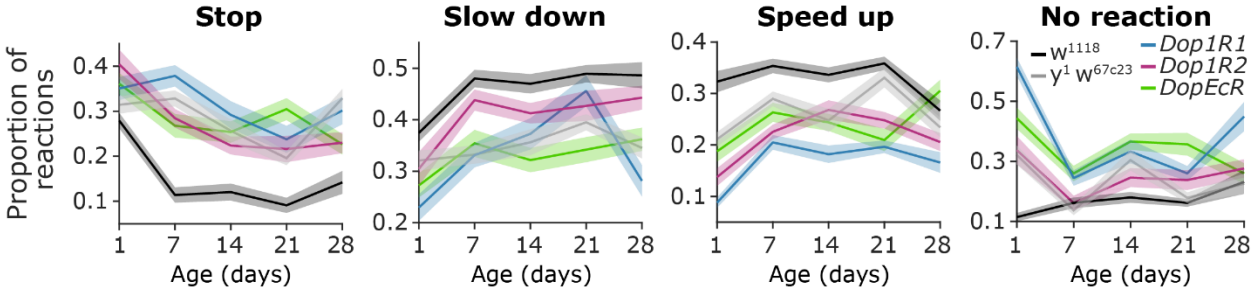


801

802

## Supplementary Figures

### Figure S1

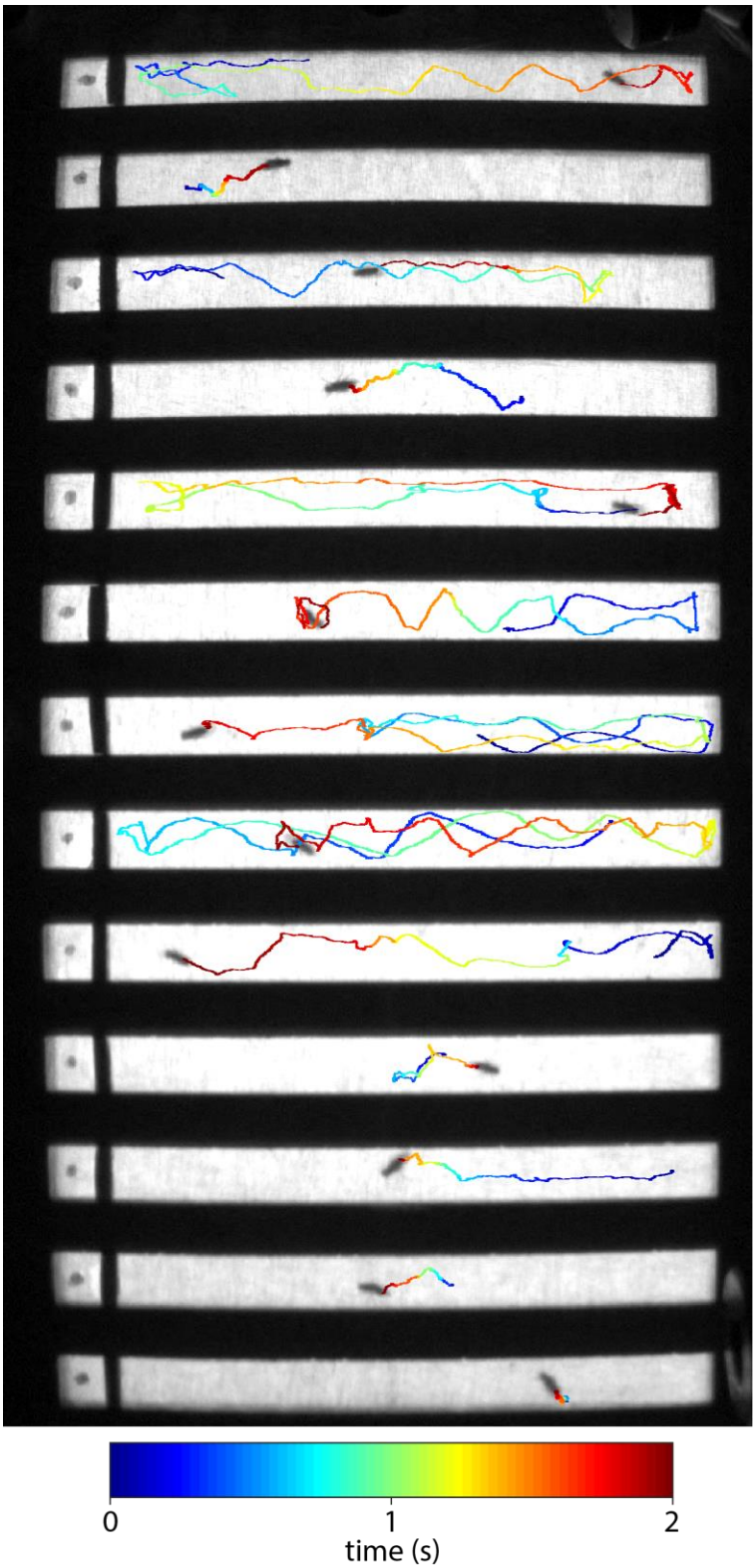

**Figure S2**

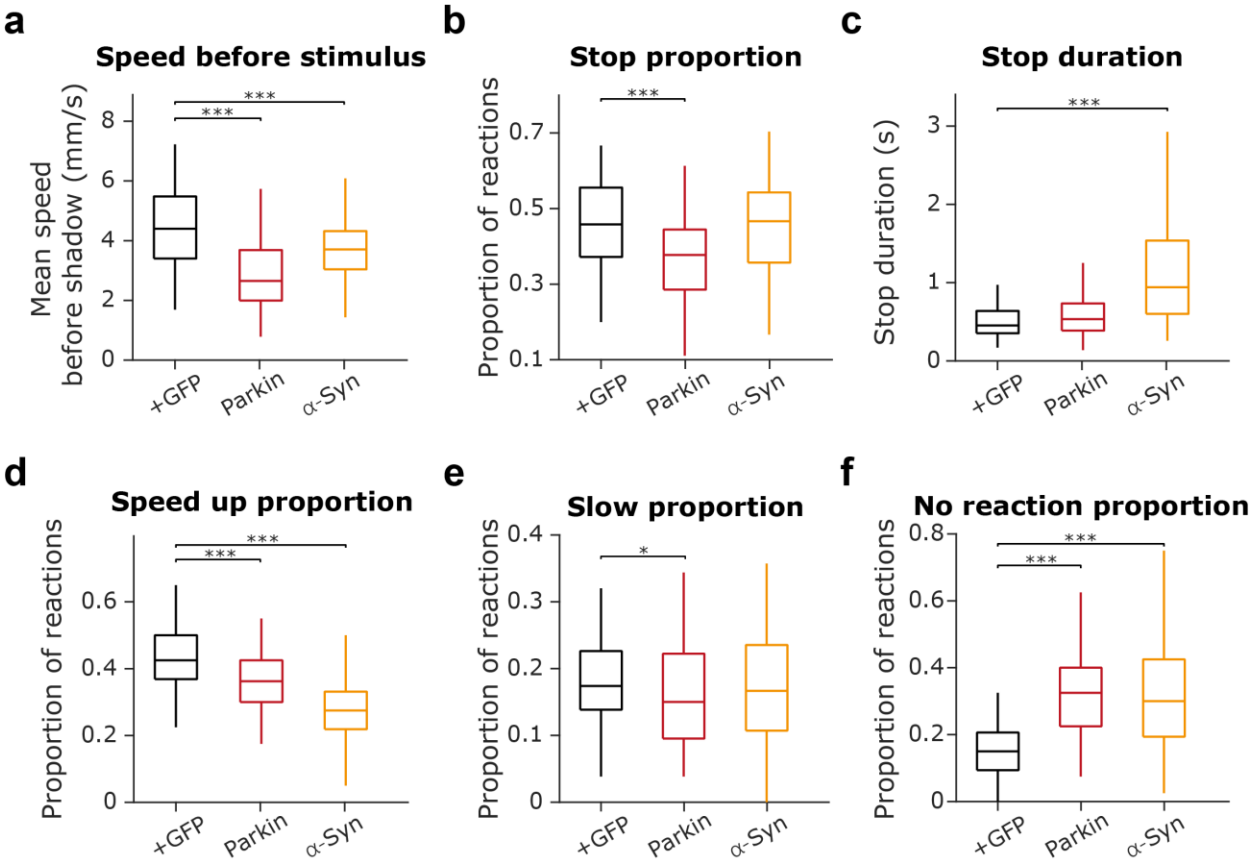
a
Speed before stimulus
Mean speed before shadow (mm/s)
0
2
4
6
8
***
***
+GFP
Parkin
α-Syn
b
Stop proportion
Proportion of reactions
0.1
0.3
0.5
0.7
***
+GFP
Parkin
α-Syn
c
Stop duration
Stop duration (s)
0
1
2
3
***
+GFP
Parkin
α-Syn
d
Speed up proportion
Proportion of reactions
0
0.2
0.4
0.6
***
***
+GFP
Parkin
α-Syn
e
Slow proportion
Proportion of reactions
0
0.1
0.2
0.3
0.4
*
+GFP
Parkin
α-Syn
f
No reaction proportion
Proportion of reactions
0
0.2
0.4
0.6
0.8
***
***
+GFP
Parkin
α-Syn

**Figure S3**

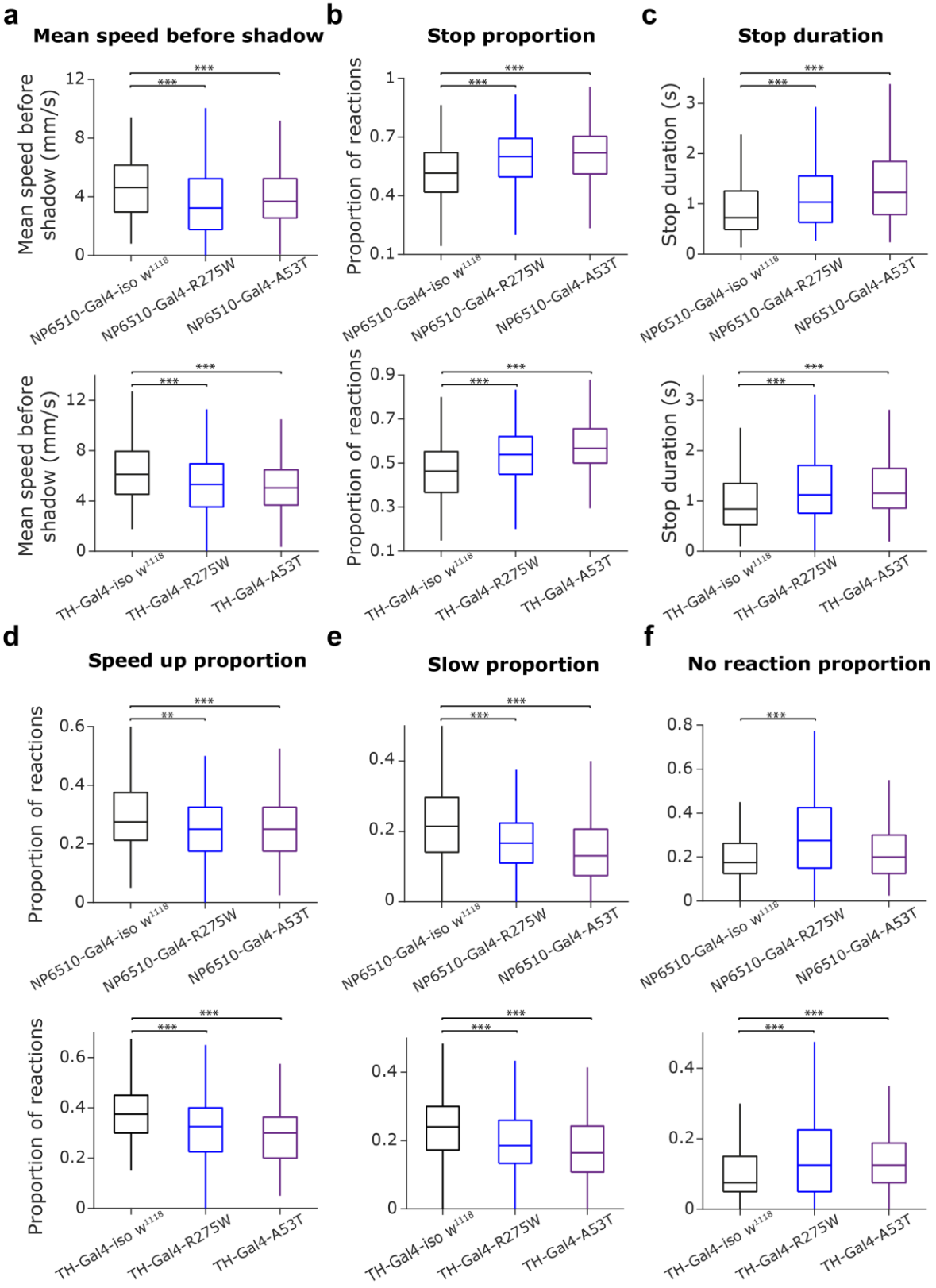
a
Mean speed before shadow
Mean speed before shadow (mm/s)
b
Stop proportion
Proportion of reactions
c
Stop duration
Stop duration (s)
NP6510-Gal4-iso w1118
NP6510-Gal4-R275W
NP6510-Gal4-A53T
TH-Gal4-iso w1118
TH-Gal4-R275W
TH-Gal4-A53T
d
Speed up proportion
e
Slow proportion
f
No reaction proportion
***
**

**Figure S4**

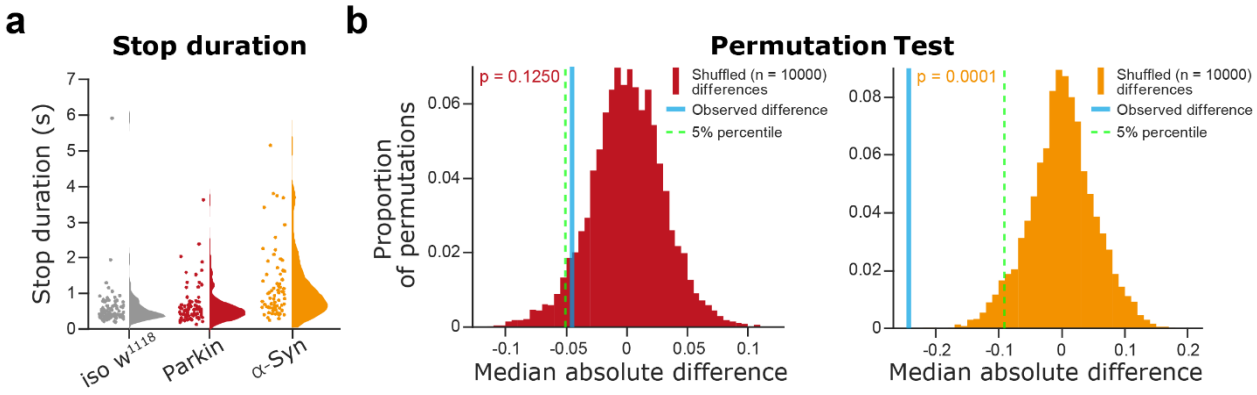
a
Stop duration
Stop duration (s)
iso w1118
Parkin
α-Syn
b
Permutation Test
p = 0.1250
Shuffled (n = 10000) differences
Observed difference
5% percentile
Proportion of permutations
Median absolute difference
p = 0.0001
Shuffled (n = 10000) differences
Observed difference
5% percentile
Median absolute difference

813 **Figure S5**

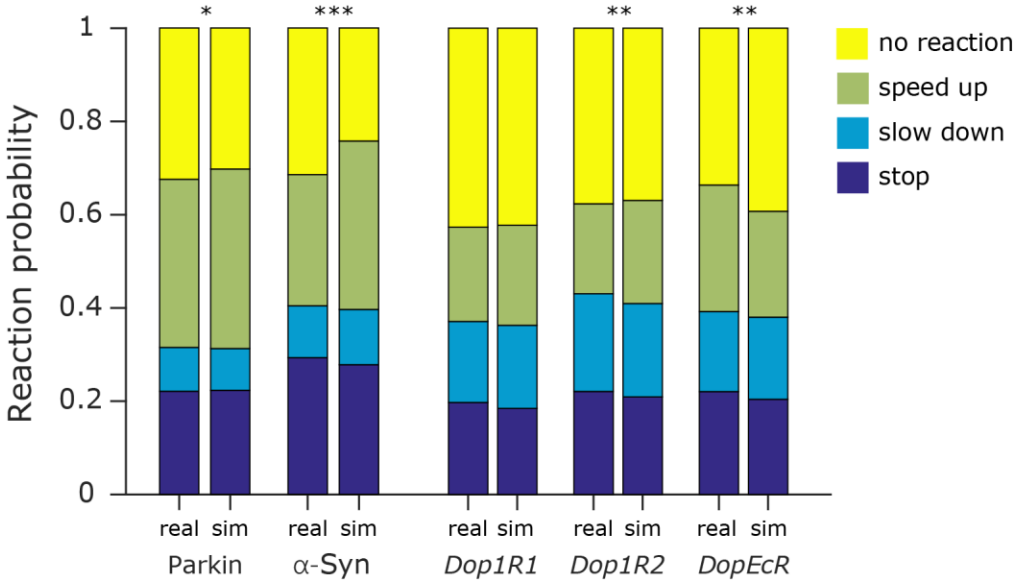


814

815

**Figure S6**

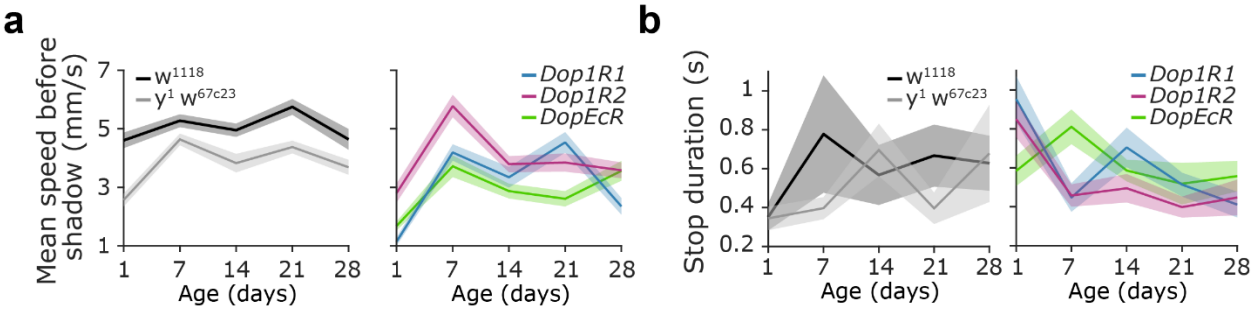
a
Mean speed before shadow (mm/s)
7
5
3
1
w1118
y1 w67c23
1 7 14 21 28
Age (days)
Dop1R1
Dop1R2
DopEcR
1 7 14 21 28
Age (days)
b
Stop duration (s)
1
0.8
0.6
0.4
0.2
w1118
y1 w67c23
1 7 14 21 28
Age (days)
Dop1R1
Dop1R2
DopEcR
1 7 14 21 28
Age (days)